Check for updates

JOURNAL OF QUATERNARY SCIENCE (2025) 1–19 ISSN 0267-8179. DOI: 10.1002/jqs.3722

JQS Journal of Quaternary Science QRA Quaternary Research Association

Stratigraphy and geomorphology of Des-Cubierta Cave (Pinilla del Valle, Madrid, Spain): Geological insights into a Neanderthal symbolic accumulation of large crania

DAVID MANUEL MARTÍN-PEREA,[1,2,3]* ENRIQUE BAQUEDANO,[3,4] JUAN LUIS ARSUAGA,[1,5] CÉSAR LAPLANA,[4] ANA ISABEL ORTEGA,[6] LUCÍA VILLAESCUSA,[4,7] BELÉN MÁRQUEZ,[4] ROSA HUGUET,[8,9,10,11] ABEL MOCLÁN,[3,11] SANDRA GÓMEZ SOLER,[4,7,12] XABIER ARROYO,[13] LAURA RODRÍGUEZ,[14,15] REBECA GARCÍA-GONZÁLEZ,[15] M. CRUZ ORTEGA,[5] JESÚS MASA-ANDRÉS,[1] DIEGO J. ÁLVAREZ-LAO,[16] NURIA GARCÍA,[1,5] M. ÁNGELES GALINDO-PELLICENA,[4] TOM HIGHAM[17,18,19] and ALFREDO PÉREZ-GONZÁLEZ[3]

[1]Department of Geodynamics, Stratigraphy, and Palaeontology, Faculty of Geology, Complutense University of Madrid, Madrid, Spain
[2]Geoarchaeology Unit, Institut Català de Paleoecologia Humana i Evolució Social (IPHES-CERCA), Tarragona, Spain
[3]Institute of Evolution in Africa—IDEA, University of Alcalá de Henares, Madrid, Spain
[4]Museo Arqueológico y Paleontológico de la Comunidad de Madrid, Alcalá de Henares, Madrid, Spain
[5]UCM-ISCIII Research Centre for Human Evolution and Behaviour, Madrid, Spain
[6]National Research Centre for Human Evolution (FA-CENIEH), Burgos, Spain
[7]Department of History and Philosophy, University of Alcalá de Henares, Madrid, Spain
[8]Institut Català de Paleoecologia Humana i Evolució Social (IPHES-CERCA), Tarragona, Spain
[9]Department of History and Art History, Rovira I Virgili University, Tarragona, Spain
[10]Unit associated to CSIC, Palaeobiology Department, National Natural Sciences Museum – CSIC, Madrid, Spain
[11]PALEVOPRIM Lab, UMR 7262, CNRS and Université de Poitiers, Potiers, France
[12]Archaeological Micromorphology and Biomarkers Laboratory (AMBi Lab), Instituto Universitario de Bio-orgánica "Antonio González", La Laguna University, Tenerife, Spain
[13]Geological Techniques Unit, Archaeology and Earth Sciences, Complutense University of Madrid, Madrid, Spain
[14]Área de Antropología Física. Departamento de Biodiversidad y Gestión Ambiental, Universidad de León. Facultad de Ciencias Biológicas y Ambientales. Campus De Vegazana, León, Spain
[15]Laboratorio de Evolución Humana, Facultad de Humanidades y Comunicacion, Universidad de Burgos, Burgos, Spain
[16]Geology Department, Oviedo University, Oviedo, Spain
[17]Oxford Radiocarbon Accelerator Unit, Research Laboratory for Archaeology and the History of Art, University of Oxford, Oxford, UK
[18]Department of Evolutionary Anthropology, University of Vienna, Vienna, Austria
[19]Human Evolution and Archaeological Sciences Forschungsverbund, University of Vienna, Vienna, Austria

Received 4 December 2024; Revised 15 April 2025; Accepted 2 May 2025

ABSTRACT: Des-Cubierta Cave, part of the Calvero de la Higuera complex, is situated in the intramountainous upper valley of the Lozoya River within the Guadarrama Range. The cave's geological, palaeontological, and archaeological record reveals a complex history of sedimentary and anthropogenic processes spanning hundreds of thousands of years, represented in 12 lithostratigraphic units. Among these, Unit 3 stands out for its archaeological significance, containing evidence of Neanderthal activity, including Mousterian lithic tools and an unusual assemblage of large mammal crania, which suggests symbolic behaviour. Geological data indicate that Unit 3 was deposited during cold periods (MIS 4) through multiple rockfall episodes, implying that these symbolic practices persisted across generations. The cave's geomorphology points to a possible Neanderthal entrance via a side opening created by erosion in the southern part of the cave. This study enhances our understanding of Des-Cubierta Cave's geological development and the long-term Neanderthal occupations, offering valuable insights into their symbolic and cultural behaviours. © 2025 The Authors *Journal of Quaternary Science* Published by John Wiley & Sons Ltd.

KEYWORDS: cave deposits; karst geomorphology; late pleistocene; middle palaeolithic; sedimentology

Introduction

Historically, symbolism has been argued to be a defining feature of *Homo sapiens*, relegating the activities of *Homo neanderthalensis* to those solely related to survival: hunting, processing and consuming animal resources, tool preparation, or the use of fire. However, a paradigm shift is well underway, and growing evidence suggests some Neanderthal activities go beyond mere subsistence and are associated with their symbolic world. Such evidence includes personal ornaments (Radovčić et al., 2015; Frayer, 2019; Rodríguez-Hidalgo et al., 2019; Frayer et al., 2020; Nowell and Cooke, 2021 and references therein), portable art (Rodríguez-Vidal et al., 2014; Majkić et al., 2018; Bello, 2021;

*Correspondence: David Manuel Martín-Perea, as above.
Email: davidmam@ucm.es

© 2025 The Authors *Journal of Quaternary Science* Published by John Wiley & Sons Ltd.
This is an open access article under the terms of the Creative Commons Attribution License, which permits use, distribution and reproduction in any medium, provided the original work is properly cited.

Leder et al., 2021), burials (Rendu et al., 2014; Zilhao, 2015; Balzeau et al., 2020), the use of structures intended for ceremonial purposes (Jaubert et al., 2016), and, although controversial, cave art (Hoffmann et al., 2018; Pitarch Martí et al., 2021; Ramos-Muñoz et al., 2022; Marquet et al., 2023).

The latest evidence of Neanderthal symbolic behaviour has been found in Des-Cubierta Cave (Baquedano et al., 2023), where a unique archaeological assemblage was recovered, comprising a collection of 35 crania from large mammals with some form of appendage (horns or antlers) belonging to bovines (*Bison priscus* and *Bos primigenius*), cervids (*Cervus elaphus*) and rhinoceroses (*Stephanorhinus hemitoechus*). Taxonomic, anatomical and, most importantly, taphonomic analyses of this assemblage suggest that it is likely associated with Neanderthal symbolism.

Detailed and comprehensive geoscientific studies are vital to confidently validating such claims. Geological studies accurately and meaningfully contextualise fossil remains, lithic artefacts, and other archaeologically significant materials. They are also essential to determining the site's geological history and understanding site formation processes.

Comprehensive analyses of site formation processes are essential in geoarchaeology, as they enable researchers to distinguish between primary and secondary depositional contexts, providing a clearer interpretation of past human activities (Goldberg et al., 2001; Karkanas, 2001; Goldberg and Berna, 2010; Karkanas and Goldberg, 2010; Aldeias et al., 2023). In cave environments, complex sedimentary dynamics can significantly alter the spatial and stratigraphic integrity of archaeological materials (Goldberg and Bar-Yosef, 1998; Goldberg, 2000; Goldberg and Sherwood, 2006; Marean et al., 2010; Campaña et al., 2017; Angelucci et al., 2018, 2023; Arriolabengoa et al., 2018; Campaña et al., 2022).

Des-Cubierta Cave, like many archaeological sites in karstic settings, has been shaped by a long and complex history of sedimentary infilling, speleothem growth, and erosion. To fully understand the site's geological evolution and its implications for Neanderthal activity, a detailed stratigraphic and sedimentological approach is required. The present study integrates stratigraphy, sedimentology, and geomorphological analyses to reconstruct the depositional history of Des-Cubierta Cave, providing crucial context for the interpretation of the archaeological record.

The main objectives of this study are (1) to describe in detail the different lithostratigraphic units hosted in Des-Cubierta Cave; (2) to produce detailed stratigraphic sections throughout the different areas of the karstic system; and (3) to infer sedimentary environments and site formation processes to contextualise the site's formation history. Additionally, we will discuss potential Neanderthal entrances to the cave, offering insights into their access routes and occupation dynamics within the site.

Geological and geographical context

Des-Cubierta Cave is located 70 km north of Madrid (40°55′23″ N 3°48′29″ W, 1112 m.a.s.l) and forms part of the Calvero de la Higuera complex (Fig. 1). The complex (Alférez et al., 1982; Pérez-González et al., 2008, 2010; Baquedano et al., 2010, 2012, 2014; Arsuaga et al., 2012; Karampaglidis, 2014) hosts, to date, five different archaeological sites (Fig. 2): Camino Cave (Laplana and Sevilla, 2006; Arsuaga et al., 2010, 2011; Álvarez-Lao et al., 2013; Laplana et al., 2013; Blain et al., 2014; Jimenez et al., 2024), Buena Pinta Cave (Huguet et al., 2010; Laplana et al., 2015, 2016; Mielgo et al., 2024), Des-Cubierta Cave (Baquedano et al., 2016, 2023; Galindo-Pellicena et al., 2019), Ocelado rockshelter (Baquedano et al., 2012), and Navalmaíllo rockshelter (Huguet et al., 2010; Abrunhosa et al., 2014, 2019, 2020; Arriaza et al., 2017; Blain et al., 2022; Márquez et al., 2013, 2016a, 2016b, 2017; Moclán et al., 2018, 2020, 2021, 2024).

The Calvero de la Higuera archaeological complex is an isolated cuesta-like landform formed by gently tilted Late Cretaceous dolostones in a homoclinal structure, dissected by the Valmaillo stream in the West and by an unnamed, poorly developed stream towards the East (Fig. 2). The structure dips a few degrees (20°–30°) northwest, towards the perennial Lozoya River, which is found less than 200 m north of the sites and flows eastward. The complex is located in the intramountainous upper valley of the Lozoya River, in the Guadarrama Range, a pop-up structure with a NE–SW trend, which is part of the Central System (Warburton and Alvárez, 1989; de Vicente et al., 2007). The Lozoya upper valley is a tectonic depression (pop-down) following the same trend as the surrounding pop-ups of the Guadarrama Range: Montes Carpetanos (Peñalara, 2428 m.a.s.l.) to the north and Cuerda Larga (Cabeza de Hierro, 2380 m.a.s.l.) to the south (Fig. 1B).

Geologically, the Lozoya upper valley is part of the schist-greywacke complex of the Central Iberian zone, composed of Proterozoic to Carboniferous rocks that were deformed and partly metamorphosed and intruded by different types of granitoids before the Permian (Vera, 2004). Although the primary deformation and metamorphism of the materials in the area occurred during the Carboniferous (Variscan), it was not until the Alpine Orogeny that the Lozoya Valley pop-down was formed (de Vicente et al., 2007).

The oldest rocks found in the valley (pre-Carboniferous and Ordovician) are orthogneisses, leucogranites, adamellites, granitoids, migmatites, and, to a lesser extent, schists and quartzites (Bellido et al., 1991; Arenas Martín et al., 1991). Quartz, lamprophiid, and porphyric dikes are also present (Arenas Martín et al., 1991).

Mesozoic sedimentation during the Late Cretaceous starts with gravels, sands, and clays from the Utrillas facies (Bellido et al., 1991; Fig. 3(A)). Overlying this formation, 35 m of marl, sandstones with dolomitic cement, gypsum and dolostones are found. These carbonates are found in shoaling upwards sequences, each consisting of three units: (1) a lower unit, consisting of marls deposited below the wave base; (2) a middle unit, composed of high-energy, wave-dominated carbonate bars; and (3) an upper unit, consisting of heavily cemented carbonates with abundant bioturbation which were deposited in shallow waters (Pérez-González et al., 2010; Fig. 3B).

Exokarst and endokarst development are common in these Mesozoic carbonates, producing abundant lapiaz landforms, dolines, and rock shelters and hosting a multilevel karstic system with subhorizontal conduits. Endokarst morphologies are heavily influenced by the differential weathering and erosion of the three units that compose the shallowing upwards sequences (Fig. 4). The lower marl unit (less resistant to weathering and erosion) and the middle unit (more porous and soluble) are affected more intensely by karstic processes, exhibiting greater endokarst development. These units host the most extensive chambers and perpendicular galleries (Fig. 4). Conversely, the upper unit, heavily cemented and more resistant to weathering and erosion, hinders endokarst development. This unit hosts only narrow galleries and heavily influences gallery development, producing a 2–4 m wide zigzag-shaped karstic system which runs for over 80 m (Fig. 4). Exokarst development is also heavily influenced by the differential weathering and erosion of these units. The upper unit, resistant to erosion and weathering, forms cliffs

© 2025 The Authors *Journal of Quaternary Science* Published by John Wiley & Sons Ltd.

10991417, 0, Downloaded from https://onlinelibrary.wiley.com/doi/10.1002/jqs.3722 by Universidad Complutense De, Wiley Online Library on [30/05/2025]. See the Terms and Conditions (https://onlinelibrary.wiley.com/terms-and-conditions) on Wiley Online Library for rules of use; OA articles are governed by the applicable Creative Commons License

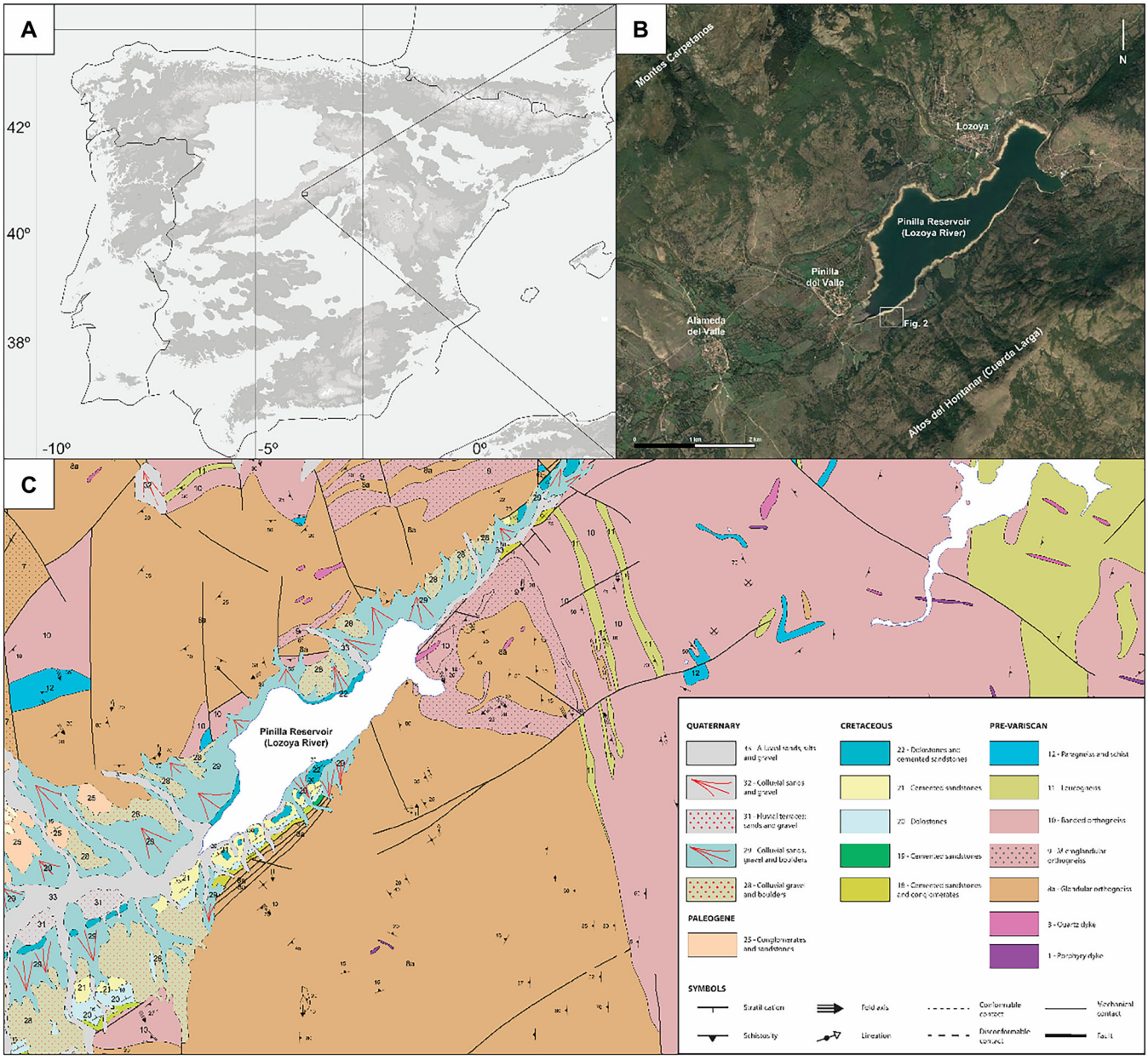

Figure 1. (A) Map of the Iberian Peninsula showing the location of the study area. (B) Orthoimage (modified from Google Earth) of the Upper Lozoya Valley, showing the mountain ranges that delimit the valley (Montes Carpetanos and Cuerda Larga), the Pinilla Reservoir and the nearby towns of Lozoya, Alameda del Valle and Pinilla del Valle. (C) Geological map of the study area. Modified from Bellido et al. (1991). [Color figure can be viewed at wileyonlinelibrary.com]

and scarps, whereas the lower and middle units, prone to erosion and weathering, undercut the cliffs and form rock shelters.

The Calvero de la Higuera multilevel karst comprises at least three subhorizontal levels: (1) at 1090 m.a.s.l., the lowermost level; (2) an intermediate level at 1105 m.a.s.l.; and (3) the uppermost known level, at 1111 m.a.s.l., which includes Des-Cubierta Cave (Baquedano et al., 2023). This uppermost level has had the roofs of all galleries and chambers dismantled by erosion.

Paleogene and Neogene fan deposits, composed mainly of polymictic conglomerates, are found throughout the Lozoya Valley, disconformably overlying previous deposits (Bellido et al., 1991). Quaternary deposits (Pleistocene and Holocene) are represented extensively in the Lozoya Valley and the surrounding mountains as fluvial terraces, alluvial fans and plains, colluvial deposits, and glacial moraines. Most importantly, Pleistocene deposits infilled the karstic landforms developed in the Mesozoic dolostones, hosting archaeological and palaeontological materials that make up the Calvero de la Higuera sites.

Materials and methods

Des-Cubierta Cave has been extensively excavated since 2009. The excavation surface extends over 90 m^2. The excavation is divided into three areas, from South to North: (1) Cubil Sector, a North–South oriented, 1/3-m-wide and 12-m-long gallery; (2) La Monumental Sector, a ~15 × 5 m chamber; and (3) Breccia Sector, a perpendicular (East–West orientation), 2/3-m-wide and 12-m-long gallery which extends over 11 m (Fig. 5).

Lithostratigraphic units were described, photographed, measured, and logged using scaled drawings. Lithostratigraphic units were described as attending to sediment texture, structure, mineralogy, colour (hue, value and chroma), and stratigraphic contacts. Colour was objectively described (hue, value and chroma) by classifying dry samples using the

© 2025 The Authors *Journal of Quaternary Science* Published by John Wiley & Sons Ltd.

10991417, 0, Downloaded from https://onlinelibrary.wiley.com/doi/10.1002/jqs.3722 by Universidad Complutense De, Wiley Online Library on [30/05/2025]. See the Terms and Conditions (https://onlinelibrary.wiley.com/terms-and-conditions) on Wiley Online Library for rules of use; OA articles are governed by the applicable Creative Commons License

Figure 2. Map of the Calvero de la Higuera archaeological complex, superimposing detailed orthoimage (Google Earth) with the topographic map (1 m contour lines), and showing the location of the archaeological sites. [Color figure can be viewed at wileyonlinelibrary.com]

Munsell Soil Colour Charts (Munsell, 1981). Eight stratigraphic sections were logged at 2–6 m spacings throughout the three excavation areas (Cubil, Monumental and Brecha Sectors).

Sediment texture was described using hand-held samples. In units where this was not possible (Units 3 and 5 to 7), representative samples were collected for granulometrical analyses from freshly scraped exposures. Sieves sized −1–4 φ were used for measuring grain size distribution. Particle size has been classified following Blott and Pye (2012).

Exposures were freshly scraped for detailed mineralogical analyses of the finer-grained units (Units 5, 6, and 8), and ~5 cm thick unaltered samples were collected. 10–15 g of each sample was homogenised by quartering and ground manually with an agate mortar until they could be entirely sieved through a 53 μm mesh.

Bulk mineralogy powder X-ray diffraction spectra (XRD) were produced using a Philipps Analytical PW 1752 Cu Kα radiation X-ray diffractometer (graphite monochromator radiation Kα1 = 1,5406 Å). Diffraction spectra were recorded continuously at 2θ angles from 2° to 68° with 0.02 stepping intervals and 1 s per step. A semiquantitative analysis was carried out using the Chung method (Chung, 1975) using EVA software.

Textural analyses of the finer-grained lithostratigraphic units were studied employing scanning electron microscopy (SEM). Small chips were extracted from each selected sample to reveal fresh fracture surfaces representative of the deposits' micro-fabric and microtexture. A gold coating was applied to these surfaces as a conductor. The SEM features an energy dispersive spectrometer (EDS) system, enabling the determination of the chemical composition of sedimentary particles during SEM observations.

In this study, the sedimentological analysis relies on facies association, which refers to groupings of facies that are spatially, texturally, and genetically linked, representing various sedimentary environments. The terms 'autochthonous' and 'allochthonous' are adopted from Iacovello and Martini (2012) and Bosch and White (2018). 'Autochthonous' denotes sediments originating from within the karstic system, such as rock fall deposits, while 'allochthonous' refers to sediments transported into the cave, like channel deposits. Chemical deposits, such as flowstones, are considered autochthonous.

Results and discussion

Cubil Sector lithostratigraphic units: Descriptions and interpretations

The Cubil Sector in Des-Cubierta Cave contains the deepest and therefore oldest deposits identified within the cave and the

© 2025 The Authors *Journal of Quaternary Science* Published by John Wiley & Sons Ltd.

10991417, 0, Downloaded from https://onlinelibrary.wiley.com/doi/10.1002/jqs.3722 by Universidad Complutense De, Wiley Online Library on [30/05/2025]. See the Terms and Conditions (https://onlinelibrary.wiley.com/terms-and-conditions) on Wiley Online Library for rules of use; OA articles are governed by the applicable Creative Commons License

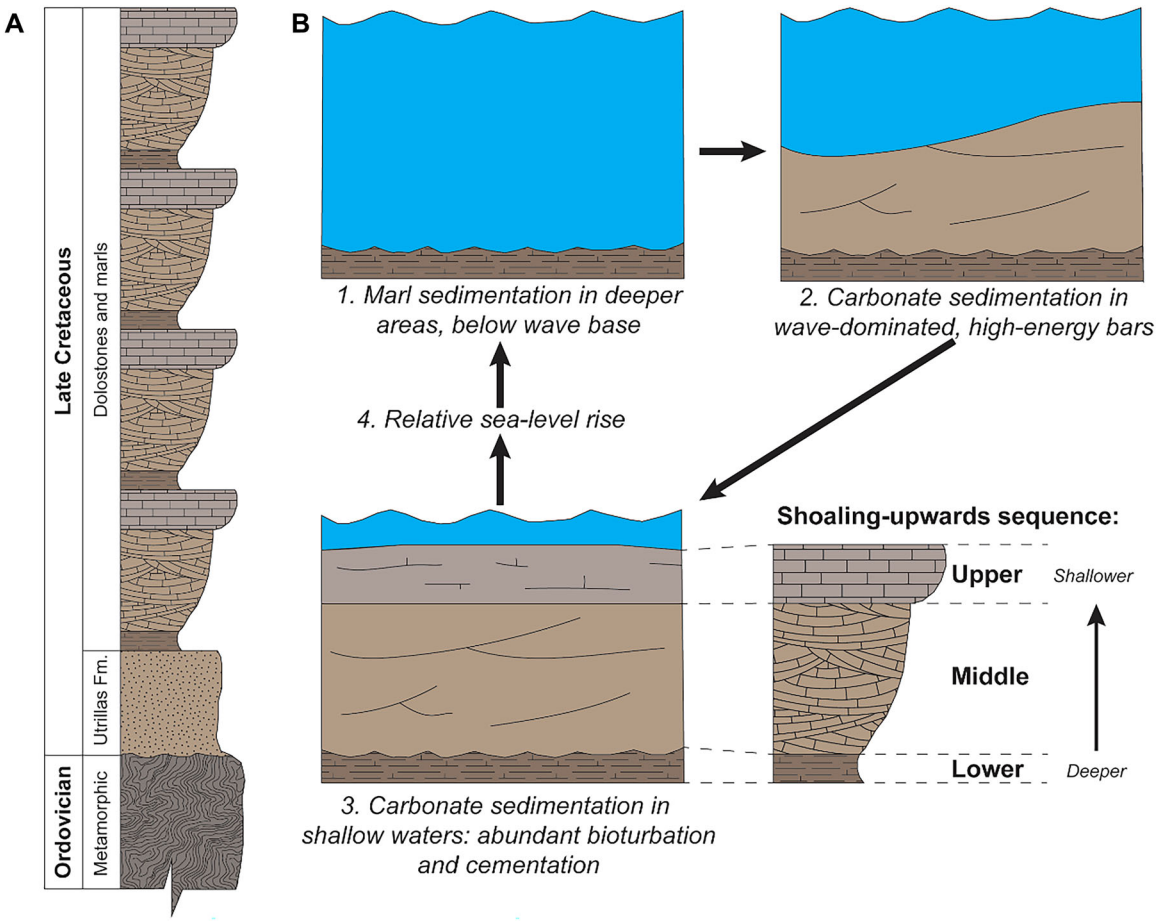

Figure 3. (A) Late Cretaceous units of the Calvero de la Higuera complex. (B) Origin of the shoaling upwards sequences, each consisting of three units: (1) a lower unit, consisting of marls deposited below the wave base; (2) a middle unit, composed of high-energy, wave-dominated carbonate bars; and (3) an upper unit, consisting of heavily cemented carbonates with abundant bioturbation which were deposited in shallow waters. Modified from Pérez-González et al. (2010). [Color figure can be viewed at wileyonlinelibrary.com]

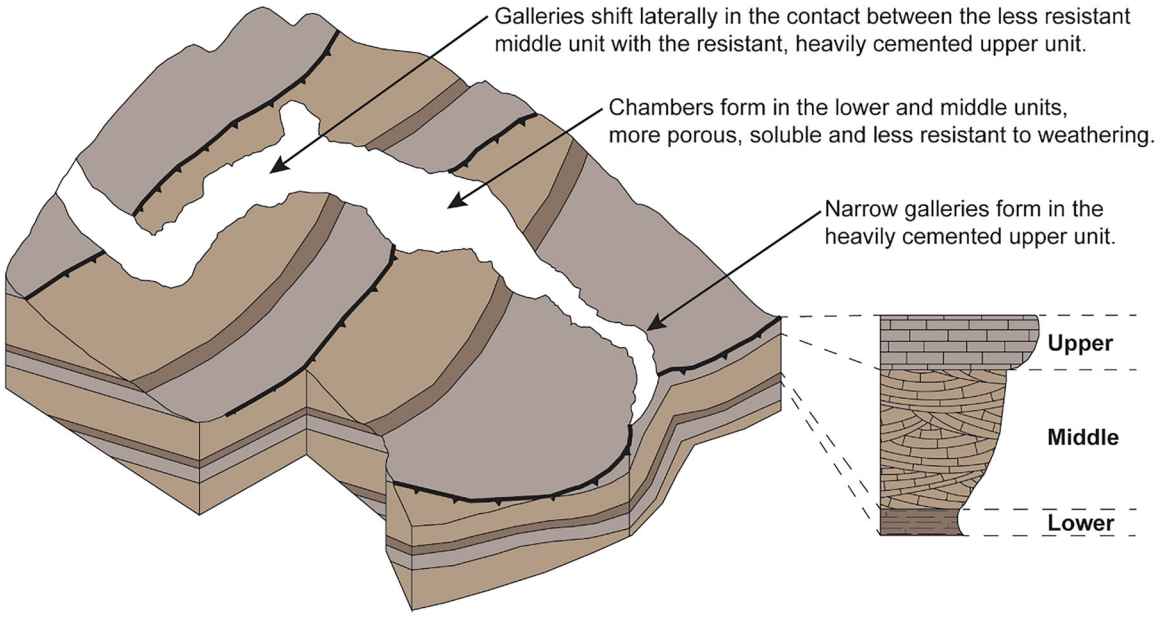

Figure 4. Petrological control of endokarst and exokarst morphologies. The lower marl unit (less resistant to weathering) and the middle unit (more porous and soluble) are affected more intensely by karstic processes, exhibiting greater endokarst development. The upper unit, heavily cemented and more resistant to weathering, hinders endokarst development and forms cliffs and scarps. [Color figure can be viewed at wileyonlinelibrary.com]

entire Calvero de la Higuera complex. The Cubil stratigraphic sections comprise eight lithostratigraphic units (Units 12 to 7, the S1 speleothem, and Unit H), described and discussed below.

Unit 12: The lowermost unit of the sequence overlays degraded limestone bedrock and consists of a 30–50 cm-thick yellow (10YR 7/8) marl deposit (Fig. 6). The sediment comprises very fine sand to silt carbonate particles and

© 2025 The Authors *Journal of Quaternary Science* Published by John Wiley & Sons Ltd.

10991417, 0, Downloaded from https://onlinelibrary.wiley.com/doi/10.1002/jqs.3722 by Universidad Complutense De, Wiley Online Library on [30/05/2025]. See the Terms and Conditions (https://onlinelibrary.wiley.com/terms-and-conditions) on Wiley Online Library for rules of use; OA articles are governed by the applicable Creative Commons License

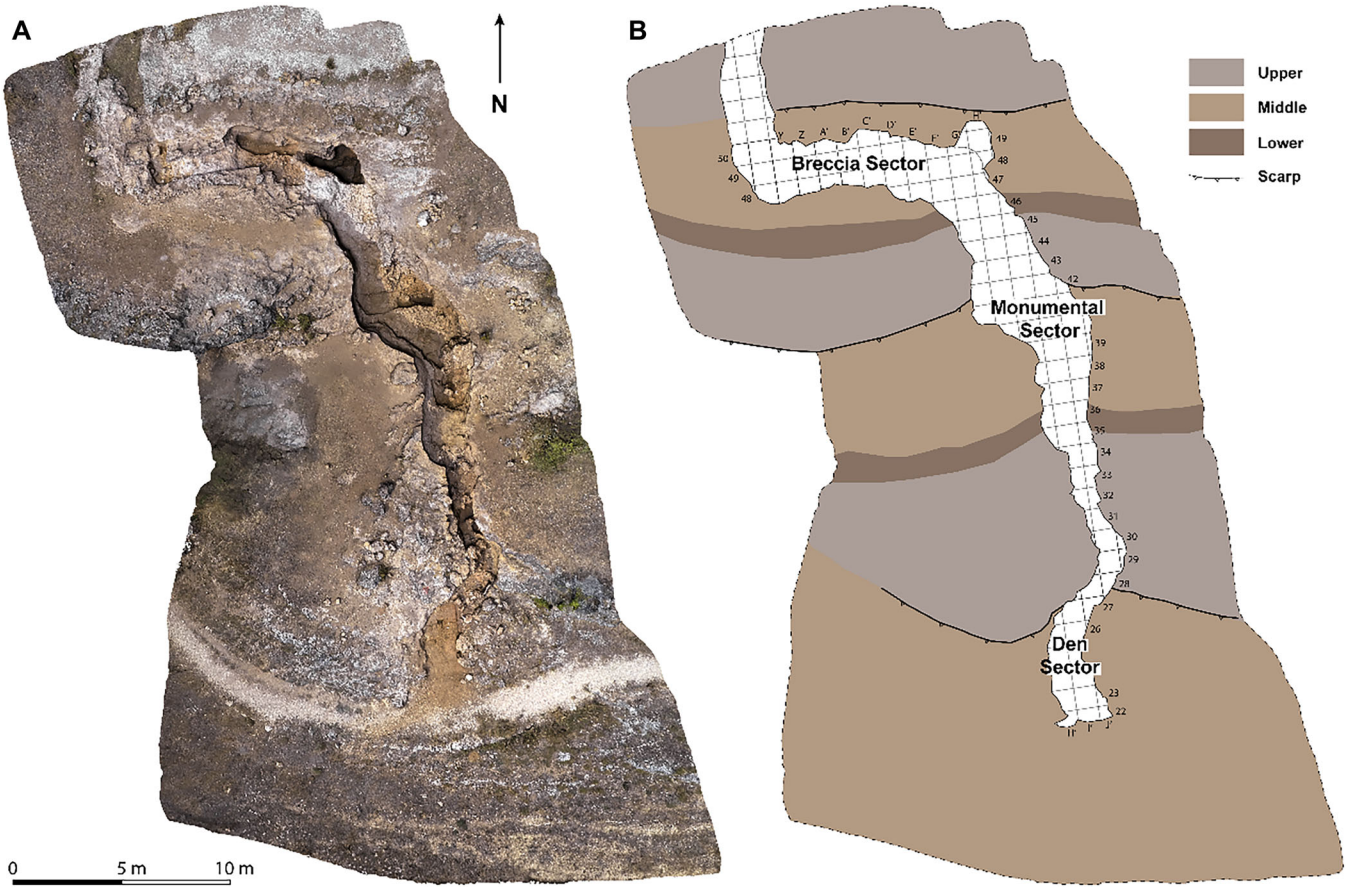

Figure 5. (A) Photogrammetric restitution of Des-Cubierta Cave. Modified from Baquedano et al., 2023. (B) Layout of the roofless cave and the excavation grid, indicating the different excavation sectors. Mesozoic units are also shown. [Color figure can be viewed at wileyonlinelibrary.com]

includes manganese oxide patches. Scattered limestone blocks are also present within the unit, likely derived from the mechanical breakdown of the cave's walls. These deposits are interpreted as backswamp facies (Bosch and White, 2018), a product of weathering and dissolution of the limestone bedrock, indicating low-energy sedimentation in a karstic environment.

Unit 11: 30–50 cm-thick pure clays with a uniform brown colour (7.5YR 5/4). Manganese oxide patches are visible within the clay. Scattered carbonate nodules, ranging in size from 0.5 to 3 cm, are also present. These features, along with the massive texture, suggest that Unit 11 was deposited in a low-energy environment, likely through slow, steady decantation processes in a backswamp setting (Gillieson, 1996; Bosch and White, 2018).

Units 12 and 11 are interpreted as backswamp facies, consisting of 'weathering residue of the bedrock and infiltrate material filtering into the conduit system from overlying soils with little or no lateral transport' (Bosch and White, 2018). Similar deposits have been documented in La Cala Cave and Oscurusciuto Rock Shelter (Martini et al., 2018, 2021), as well as in Gran Dolina Cave (Campaña et al., 2022), where fine-grained sediments accumulate in low-energy, waterlogged conditions, often reflecting prolonged periods of minimal transport and localised sedimentation.

Unit 10: Unit 10 represents a complex sequence of fining upwards sequences (Fig. 6), divided into eight sandy subunits (10.9 to 10.3 and 10.1) and a clay subunit (10.2). The basal subunits (10.9, ~25 cm thick, and units 10.8 and 10.7, both ~6 cm thick) are characterised by moderately sorted coarse to fine sand, with angular and very angular quartz, feldspar, and gneiss clasts. Subunits 10.6 to 10.4 transition to poorly sorted, very coarse sand, granules, and small pebbles. This sequence is thickening upwards, with sub-unit 10.6 being ~10 cm thick, 10.5 being 20 cm thick, and 10.4 being ~28 cm thick. The uppermost subunits (10.3, 18 cm thick, and 10.1, 12 cm thick) contain poorly sorted, very coarse sand and granules with occasional large gneiss and limestone pebbles. These subunits reflect varying depositional processes and energy levels in channel facies (Bosch and White, 2018). Unit 10 is interpreted as several episodic high-energy events followed by low-energy flooding during the waning stages. Unit 10.2 is a 40–60 cm-thick deposit of very pure clay, reddish-brown (5YR 4/4). Like Unit 11, the clay has a massive texture, suggesting deposition from suspension in a low-energy, stagnant water environment. Unit 10.2 disconformably overlies sub-units 10.3 and 10.4 over an erosive surface. Additionally, it is disconformably overlain by subunit 10.1 and paraconformably by Unit 9 (Fig. 6). The presence of abundant postdepositional carbonate nodules, likely formed during periods of subaerial exposure, suggests fluctuations in water levels and possible pedogenic processes.

This sedimentary sequence is interpreted as fluvial deposits formed by a local stream, influenced by the Lozoya River base level. Given its stratigraphic position, 23 m above the current Lozoya River channel (~1110 m.a.s.l.), these deposits can be correlated with the Middle Pleistocene T19 terrace (Karampaglidis, 2014). Terraces at this elevation above the thalweg in other parts of the Madrid Basin are dated between 300 000 and 400 000 years (Panera et al., 2011; Silva et al., 2017).

Unit 9: yellowish-brown (10YR 6/6) clays with carbonate nodules (Fig. 6). SEM observations reveal a microfabric of face-to-face contacts between smectites (Fig. 7A). These clays are interpreted as slackwater facies (Bosch and

© 2025 The Authors *Journal of Quaternary Science* Published by John Wiley & Sons Ltd.

10991417, 0, Downloaded from https://onlinelibrary.wiley.com/doi/10.1002/jqs.3722 by Universidad Complutense De, Wiley Online Library on [30/05/2025]. See the Terms and Conditions (https://onlinelibrary.wiley.com/terms-and-conditions) on Wiley Online Library for rules of use; OA articles are governed by the applicable Creative Commons License

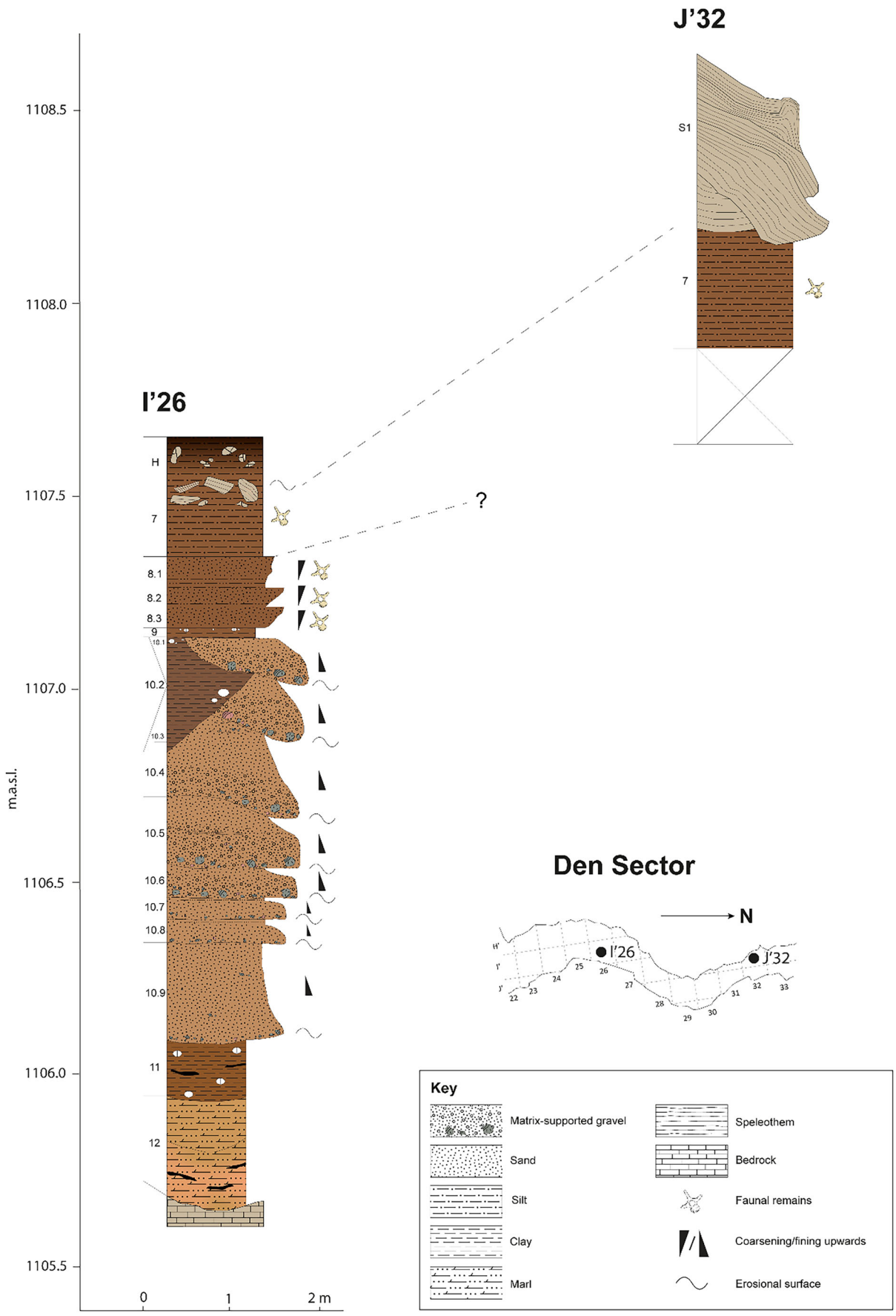

Figure 6. Detailed stratigraphic sections of Den Sector in Des-Cubierta Cave. [Color figure can be viewed at wileyonlinelibrary.com]

© 2025 The Authors *Journal of Quaternary Science* Published by John Wiley & Sons Ltd.

10991417, 0, Downloaded from https://onlinelibrary.wiley.com/doi/10.1002/jqs.3722 by Universidad Complutense De, Wiley Online Library on [30/05/2025]. See the Terms and Conditions (https://onlinelibrary.wiley.com/terms-and-conditions) on Wiley Online Library for rules of use; OA articles are governed by the applicable Creative Commons License

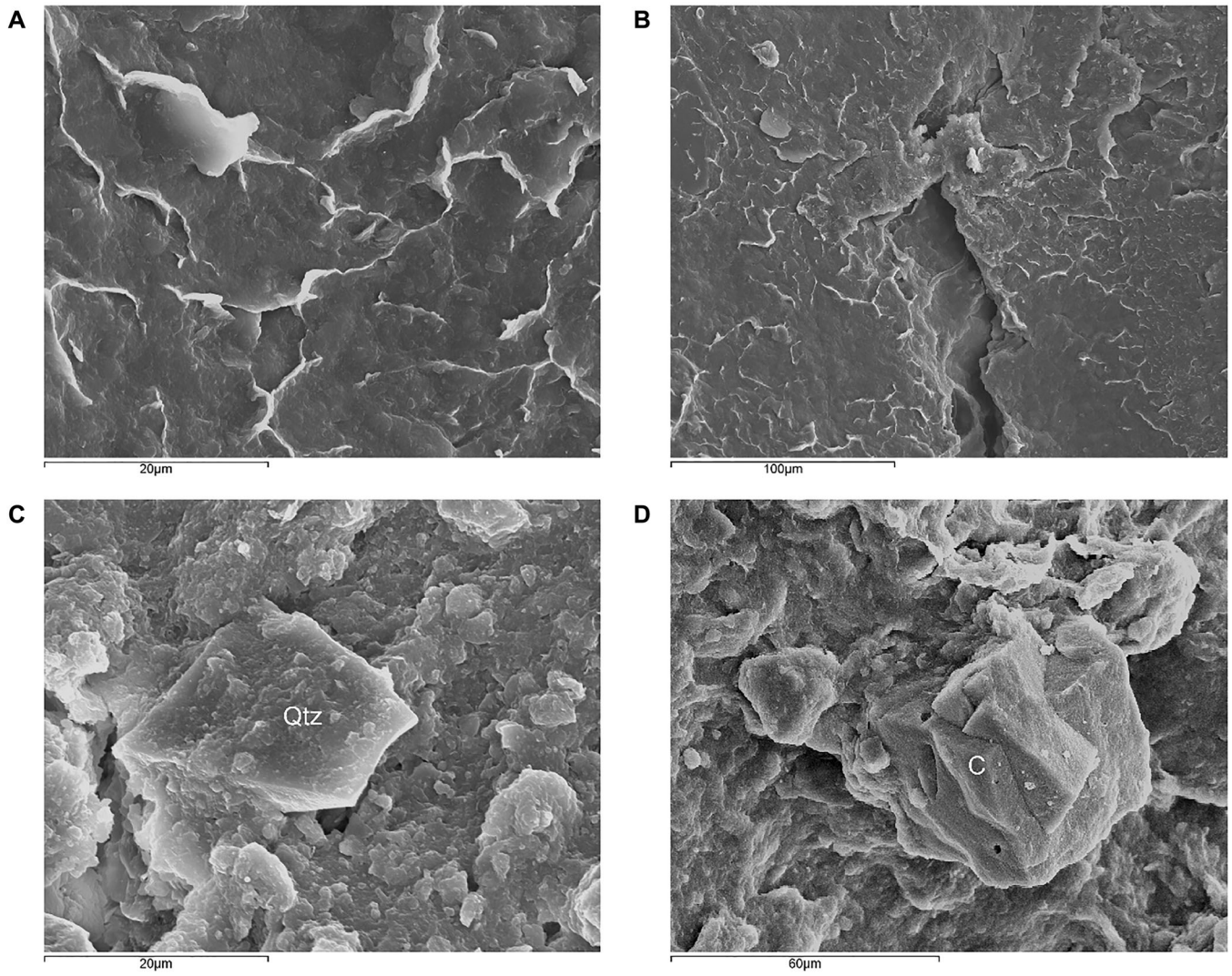

Figure 7. SEM images of representative sample chips. (A) Smectites with face-to-face contacts and some curly contacts in Unit 9 clays. (B) Smectites with face-to-face contacts in Unit 7. (C) Angular, low sphericity quartz clast in a smectite and kaolinite groundmass in Unit 8. (D) Calcite crystal in smectite and kaolinite groundmass in Unit 8.

White, 2018), product of low-energy, slow and steady decantation processes during a single fluvial flooding event. The presence of carbonate nodules indicates that these likely formed during a period of subaerial exposure after this flooding event.

Unit 8: Unit 8 consists of three coarsening-upward sequences (Fig. 6). Subunit 8.3 is a 6-cm-thick, reddish yellow (7.5YR 6/8) coarsening upwards deposit, from medium sands to poorly sorted granules. Subunit 8.2 is a 5-cm-thick, reddish yellow (7.5YR 6/8) coarsening upwards deposit, from medium sands to poorly sorted granules. Subunit 8.1 is an 8-cm-thick, reddish yellow (7.5YR 6/8) coarsening upwards deposit, from medium sands to poorly sorted granules. The clasts in these sequences primarily comprise quartz, feldspar and calcite, with moderate angularity and medium sphericity (Fig. 7C,D). Abundant fossil remains are found within these sequences. Based on the presence of coarsening-upward sequences, Unit 8 is interpreted as a series of flooding events, recorded as channel facies (Bosch and White, 2018). The poorly sorted sediments with angular clasts further suggest rapid, high-energy deposition typical of episodic flooding events.

Units 10 and 8 are interpreted as channel deposits (Bosch and White, 2018). These common cave-interior deposits are also documented nearby in Camino Cave (Pérez-González et al., 2010) and in other karstic systems in the Iberian plateau (Aranburu et al., 2017; Campaña et al., 2017, 2022; Laborda et al., 2024).

Unit 7: 20 cm-thick reddish yellow (7.5YR 6/8) sandy silty clay (Tables 1 and 2, Fig. 8, Appendix S1) with some scarce floating subrounded, low sphericity dolostone coarse gravel clasts. The deposit is massive and lacks significant internal structures, typical of slackwater facies (Bosch and White, 2018), suggesting deposition by low-energy water processes such as flooding. Supporting this interpretation, observed microfabrics with face-to-face contacts (Fig. 7B) are indicative of flocculated clay minerals deposited in low-energy sedimentary processes. Unit 7 also contains fossil remains. The top of the unit shows evidence of intense erosion.

S1 speleothem: S1 is a 40 to 50-cm thick calcite flowstone (Table 3) precipitated over Unit 7. The speleothem is complete and laterally continuous towards the north. Still, it is heavily eroded in the southern area, where it is found as isolated small to large boulders in the erosive contact between Unit 7 and the Holocene Ap soil horizon, referred to as Unit H, described below. Five U-Th dates indicate that the uppermost 10 cm of the speleothem formed throughout MIS7 (Baquedano et al., 2023). These datings place the underlying Units 7–12 in the Middle Pleistocene.

Unit H: 10–20 cm-thick brown to dark brown (7.5YR 4/3 to 7.5YR 3/3) Ap soil horizon disconformably overlying Unit 7

© 2025 The Authors *Journal of Quaternary Science* Published by John Wiley & Sons Ltd.

10991417, 0, Downloaded from https://onlinelibrary.wiley.com/doi/10.1002/jqs.3722 by Universidad Complutense De, Wiley Online Library on [30/05/2025]. See the Terms and Conditions (https://onlinelibrary.wiley.com/terms-and-conditions) on Wiley Online Library for rules of use; OA articles are governed by the applicable Creative Commons License

Table 1. XRD results for the studied samples, showing the Reference Intensity Ratios of the existing phases, allowing the intensity calculations to be normalised on the assumption that the sum of all phases in the sample is equal to 100%.

	Quartz	Plagioclase	K Feldspar	Filosilicate	Calcite	Dolomite	Siderite	Apatite
Unit 3.1	14	5	5	10	18	48	-	-
Unit 3.1	19	7	5	14	12	43	-	-
Unit 5	11	5	13	12	12	42	-	5
Unit 5	24	1	28	19	12	11	-	5
Unit 6	37	-	15	21	15	-	5	7
Unit 7	35	-	26	37	-	2	-	
Unit 7	28	-	16	32	19	3	-	2
Unit 8	28	-	40	29	-	-	3	
Unit 9	26	-	25	49	-	-	-	

Table 2. Oriented aggregates abundance results.

	Smectite	Mica-Illite	Clorite	Kaolinite
Unit 3.1	*	**	*	**
Unit 5	*	**	*	**
Unit 6	*	**	*	**
Unit 7	*	**	*	**
Unit 7	*	**	*	**
Unit 8	*	**	*	**
Unit 9	*	**	*	**

*: Not abundant. **: Abundant.

over an erosive surface. Unit H contains abundant angular limestone and dolostone cobbles and boulders (Fig. 6).

Monumental Sector lithostratigraphic units: Descriptions, interpretations, and correlations

The excavation of the Monumental Sector has not been completed, and the bottom of the gallery has not been reached. This sector comprises 10 lithostratigraphic units (Fig. 9), including Unit 7 and the S1 speleothem, which were previously described in the Cubil Sector. The following sections provide detailed descriptions and discussions of each lithostratigraphic unit.

Unit 7: Unit 7 is the oldest and deepest excavated unit in the Monumental sector, though it has only been exposed in the centremost, widest section of the cave. This unit consists of light reddish-brown (5YR 6/4) sandy silty clay (Tables 1 and 2, Appendix S1), more than 150 cm thick, with thin interspersed lenses of sand containing scarce granules. The unit's base has not been exposed, while its upper contact is marked by an eastward-dipping erosional surface, indicating significant postdepositional modification, likely caused by hydrodynamic processes within the cave system.

S1 speleothem: In this area of the cave, S1 is 20 to 40 cm thick. This flowstone is laterally continuous across the narrow sections of the cave but is found as small to large boulders in wider areas, in between the erosive contact between Units 7 and 6 (Fig. 10). This suggests a period of significant erosion which partially eroded the underlying Level 7 and caused the speleothem to collapse gravitationally. The precipitation of S1 likely reflects stable, warm environmental conditions, with sufficient water flow to sustain calcite precipitation over an extended period.

Unit 6: Unit 6 is composed of a light reddish-brown (5YR 6/4) sandy silty clay deposited overlying collapsed fragments of the S1 speleothem. The unit rests on an eastward-dipping erosional surface (Fig. 10A). The fine-grained, massive texture of the deposit is interpreted as slackwater facies (Bosch and White, 2018). It suggests slow sediment accumulation, likely driven by low-energy fluvial processes. Unit 6 is eroded by another eastward-dipping erosional surface, where a gour surface has developed due to partial cementation of the clay sediments (Fig. 10B).

Unit 5: Disconformably overlying the gour surface is Unit 5, a 30–45 cm-thick deposit of light reddish-brown (5YR 6/4) sandy silty clay with thin lenses of sand and very fine gravel. The deposit is interpreted as slackwater facies (Bosch and White, 2018), with sand and very fine gravel lenses indicating episodic higher-energy events, likely flash floods that introduced coarser material into the cave.

Units 9, 7, 6, and 5 are interpreted as slackwater facies (Bosch and White, 2018), which are commonly found in karstic caves (Bull, 1981; Springer & Kite, 1997; Auler et al., 2009; Martini, 2011; Iacoviello and Martini, 2012; Laureano et al., 2016; Martín-Perea et al., 2022; Campaña et al., 2022). These facies are typically associated with periodic flooding events that lead to the deposition of fine-grained sediments in low-energy cave environments (Bull, 1981; Herman et al., 2012).

S2 speleothem: The S2 speleothem is a thin (1–4 cm) flowstone layer that precipitated over the S1 speleothem in areas where it remains in situ and over Unit 5 in regions where S1 has collapsed. S2 is also overlain by the growth of several stalagmites, particularly in the central and widest sections of the cave. U-Th dating of one of these stalagmites provided an age of 135.7 ± 1.9 ka (Baquedano et al., 2023).

Unit 4: Unit 4 is a 10–15 cm-thick clast-supported gravel deposit consisting primarily of flat, angular, rectangular prism limestone and dolostone cobbles and boulders (Fig. 10A). These gravels are embedded in a scant carbonatic clayey silt matrix. Prismatic, angular clasts and the scarcity of matrix suggest that this unit represents in situ breakdown material from the cave walls and roof (rockfall facies; Gillieson, 1996; White, 2007), likely associated with frost weathering and gravitational collapse during colder periods.

Unit 3: Unit 3 consists of a very pale brown (10YR 8/4), clast-supported to open framework gravel deposit, primarily composed of limestone and dolostone angular to subangular cobbles and boulders with a scant carbonatic silty matrix (Table 5, Appendix S1), interpreted as rockfall facies (Gillieson, 1996; White, 2007). Towards the north and south of the cave, Unit 3 rests conformably over the S1 speleothem, whereas it lies on top of Unit 4 in the centre of the cave. This unit is up to 2 m thick in the centremost area of the cave and gradually thins out towards the north and south.

This conic shape has its apex in the sector's centremost part, where the cave is the widest. This geometry suggests the presence of an opening (collapse doline) directly above the apex, allowing rockfall material to accumulate below (Fig. 12(G)). The inferred opening aligns with the contact

© 2025 The Authors *Journal of Quaternary Science* Published by John Wiley & Sons Ltd.

10991417, 0, Downloaded from https://onlinelibrary.wiley.com/doi/10.1002/jqs.3722 by Universidad Complutense De, Wiley Online Library on [30/05/2025]. See the Terms and Conditions (https://onlinelibrary.wiley.com/terms-and-conditions) on Wiley Online Library for rules of use; OA articles are governed by the applicable Creative Commons License

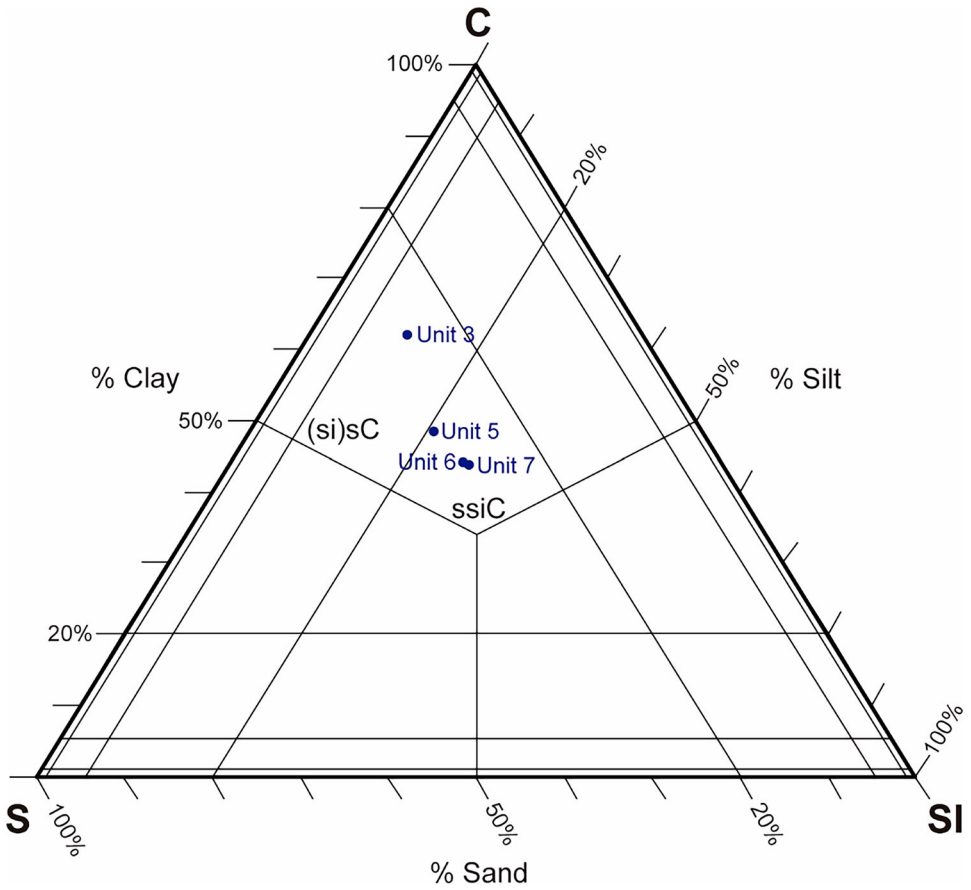

Figure 8. Units 3 and 5 to 7 granulometries projected on ternary diagrams, according to Blott and Pye (2012). (si)sC: very slightly silty, sandy clay; ssiC: sandy silty clay. [Color figure can be viewed at wileyonlinelibrary.com]

Table 3. XRD results for the studied speleothems, showing the Reference Intensity Ratios of the existing phases, allowing the intensity calculations to be normalised on the assumption that the sum of all phases in the sample is equal to 100%.

	Quartz	Plagioclase	K Feldspar	Filosilicate	Calcite	Aragonite	Dolomite	Gypsum
S2 speleothem	16	5	4	11	44	0	20	0
E2 speleothem	1	4	0	0	92	0	2	1
E1 speleothem	2	7	0	4	31	8	48	0
S1 speleothem	4	4	2	0	87	0	3	0
S1 speleothem	1	5	0	0	91	0	1	2

between the Cretaceous upper and middle units, indicating that the cave was open to the exterior during the deposition of these rockfall deposits.

Unit 3 contains evidence of Neanderthal activity, including Mousterian lithic tools such as anvils, hammerstones, cores, and flakes (Baquedano et al., 2023). Additionally, the faunal remains are dominated by large ungulates, mainly bovines, alongside some cervids and steppe rhinoceroses, with an unusual concentration of cranial remains. These crania, often directly associated with anvils and hammerstones, have been interpreted as evidence of symbolic behaviour rather than a subsistence practice (Baquedano et al., 2023).

The sedimentological characteristics, combined with the evidence from pollen and micromammal assemblages (Baquedano et al., 2023), indicate that this level formed during a cold climatic phase. Direct dating was attempted on multiple bone samples from Unit 3, but all lacked sufficient collagen for successful analysis. Given these limitations, the formation age of Unit 3 must be inferred from the dating of adjacent lithostratigraphic units. The oldest possible age for this layer is determined by the dating of the underlying S2 speleothem, corresponding to the end of MIS6. Although MIS 5 is not homogeneous and includes colder substages such as MIS 5 d and 5b, these phases were generally milder compared to MIS 4, which is characterised by sustained cold conditions. The ecological and sedimentological data from this level suggest a colder climate, making MIS 4 the most plausible depositional timeframe for Unit 3.

Given the inferred depositional environment, sedimentary processes, and the substantial thickness of Unit 3, the deposit is likely multiepisodic, formed through multiple phases of rockfall and sediment accumulation. Additionally, these depositional events could have occurred over an extended period throughout MIS4. Since geological evidence points to a prolonged and multiphase deposition, it could have profound implications for archaeological interpretations. It would suggest that the Neanderthal symbolic practices were not isolated incidents, but behaviours maintained and transmitted across multiple generations. Future research, particularly involving detailed spatial analyses of the archaeological remains, should explore this possibility to better understand the continuity of these cultural practices within Unit 3.

Unit 2: Unit 2 lies on an onlap over Unit 3, consisting of a light reddish brown (5YR 6/4) clast-supported gravel deposit

© 2025 The Authors *Journal of Quaternary Science* Published by John Wiley & Sons Ltd.

10991417, 0, Downloaded from https://onlinelibrary.wiley.com/doi/10.1002/jqs.3722 by Universidad Complutense De, Wiley Online Library on [30/05/2025]. See the Terms and Conditions (https://onlinelibrary.wiley.com/terms-and-conditions) on Wiley Online Library for rules of use; OA articles are governed by the applicable Creative Commons License

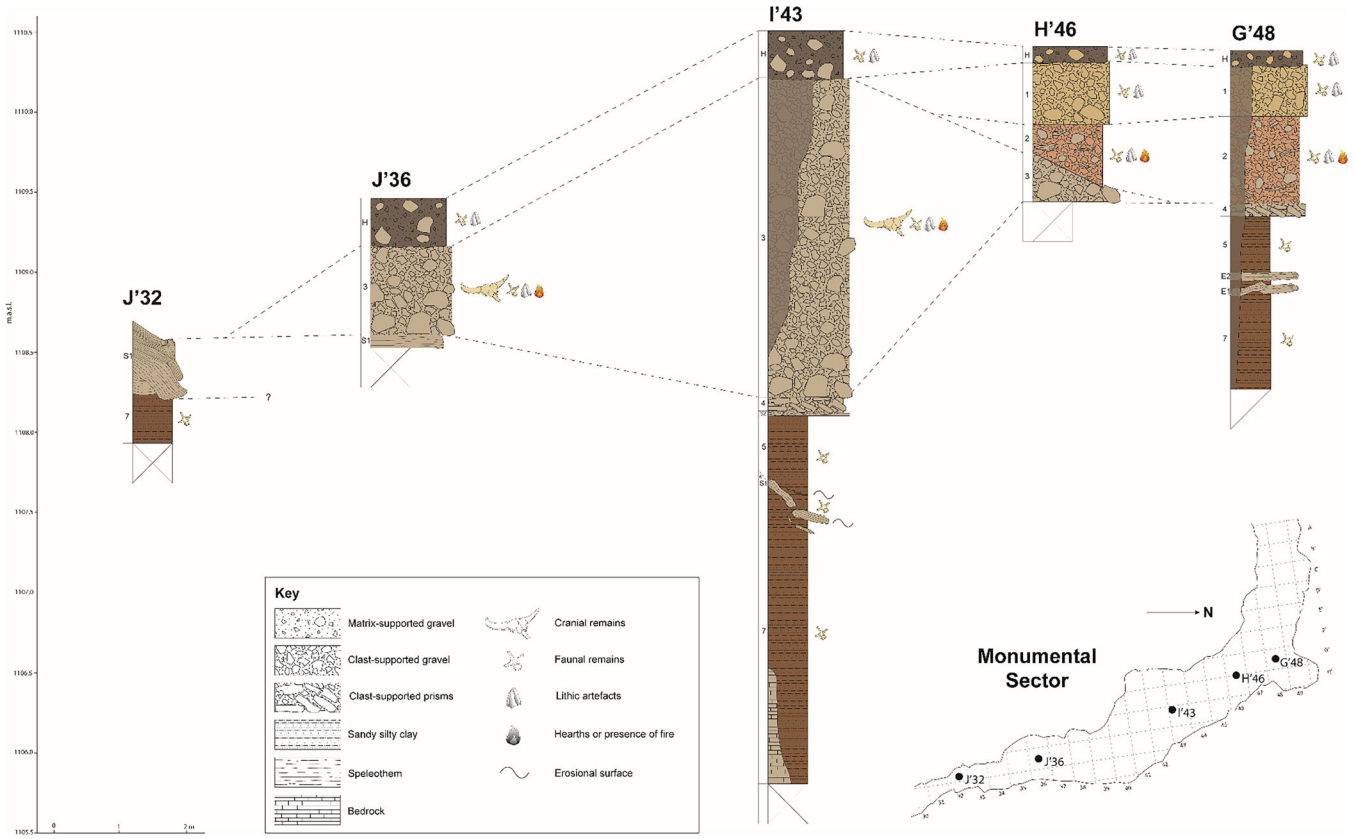

Figure 9. Detailed stratigraphic sections of Monumental Sector in Des-Cubierta Cave. Modified from Baquedano et al. (2023). [Color figure can be viewed at wileyonlinelibrary.com]

heavily cemented with carbonate. The gravels are heterometric, containing rounded and sub-rounded limestone and dolostone pebbles and cobbles within an allochthonous silty sand matrix (Table 4). Occasional thin, laminated speleothem fragments are embedded within the deposit. The maximum thickness of this unit is 55 cm in the northern section, thinning towards the south, forming an onlap with Unit 3. This unit is interpreted as rockfall facies (Gillieson, 1996; White, 2007), formed due to the progressive erosion of the cave walls, including parietal speleothems. The presence of an allochthonous matrix suggests an open-cave setting, where wind-borne silts and sands could percolate between the breakdown clasts.

Unit 2 also contains archaeological material, including a Neanderthal mandible, faunal remains, Mousterian lithic artefacts and combustion structures. A radiocarbon dated charcoal fragment, with a calibrated date (95.4% probability) ranging from 43 400 to 52 960 cal BP (84.6%) and extending up to 53 150 cal BP beyond the dating range (10.9%), suggests a minimum age around the middle of MIS3. The pollen found in Unit 2 indicates mild and humid conditions, suggesting that this layer was deposited during a warm phase within the generally cold period of MIS4 or MIS3 (Baquedano et al., 2023).

Unit 1: Unit 1 comprises an intensely cemented light brown (7.5YR 6/4) clast-supported gravel deposit. The gravels consist of heterogeneously sized limestone and dolostone pebbles, cobbles, and boulders within a silty sand carbonatic and quartz-feldspathic matrix (Table 4). This unit is up to 40 cm thick and lies conformably over Level 2, gradually pinching out towards the south. This unit is interpreted as rockfall facies (Gillieson, 1996; White, 2007) and represents the final stages of denudation and erosion of the cave. The original cave structure had largely disintegrated at this stage, leaving only remnants subject to continued denudation.

Units 4-1 are interpreted as breakdown deposits in rockfall facies, one of the most common deposits in caves (Gillieson, 1996; White, 2007). These facies are found in other sites in the Calvero de la Higuera complex, such as Navalmaíllo Rockshelter and Camino Cave (Pérez-Gonzalez et al., 2010), and in nearby karstic archaeological sites (Campaña et al., 2017; Álvarez-Alonso et al., 2018; Campaña et al., 2022).

Unit H: The uppermost level, Unit H, consists of a 10–80 cm thick dark brown (7.5YR 3/3) Ap soil horizon that disconformably overlies Units 1 and 3. The soil horizon includes reworked fossil material from these underlying units. Unit H is also found penetrating all the underlying units due to a present-day sink located in the eastern, lowermost part of the Monumental Sector. This sink aligns with the more erodible and less resistant Late Cretaceous marl Lower Unit, allowing for the downward infiltration of water and sediments.

Breccia Sector lithostratigraphic units: Descriptions, interpretations and correlations

The Breccia Sector represents the final area of Des-Cubierta Cave. As the most recent area to undergo excavation, substantial portions of this part of the gallery remain to be explored. In this sector, two additional lithostratigraphic units and three speleothems have been identified alongside previously described units (Units 7, 5, 4, 2, 1, and H) from the Monumental Sector (Fig. 11). The following section offers descriptions and discussions of each lithostratigraphic unit.

E1 and E2 speleothems: Located in the easternmost and deepest area of the Breccia Sector are two 10–15 cm thick flowstones. Based on their stratigraphic position overlying Unit 7 and their mineralogical composition (Table 3), it is likely that these speleothems are part of the same formation as the S1 speleothem. Like S1, the E1 speleothem also shows evidence of partial breakage and erosion.

Unit 3.1: Unit 3.1 is a <45 cm-thick deposit of light reddish-brown (5YR 6/4) heavily cemented clast-supported gravel. The

© 2025 The Authors *Journal of Quaternary Science* Published by John Wiley & Sons Ltd.

10991417, 0, Downloaded from https://onlinelibrary.wiley.com/doi/10.1002/jqs.3722 by Universidad Complutense De, Wiley Online Library on [30/05/2025]. See the Terms and Conditions (https://onlinelibrary.wiley.com/terms-and-conditions) on Wiley Online Library for rules of use; OA articles are governed by the applicable Creative Commons License

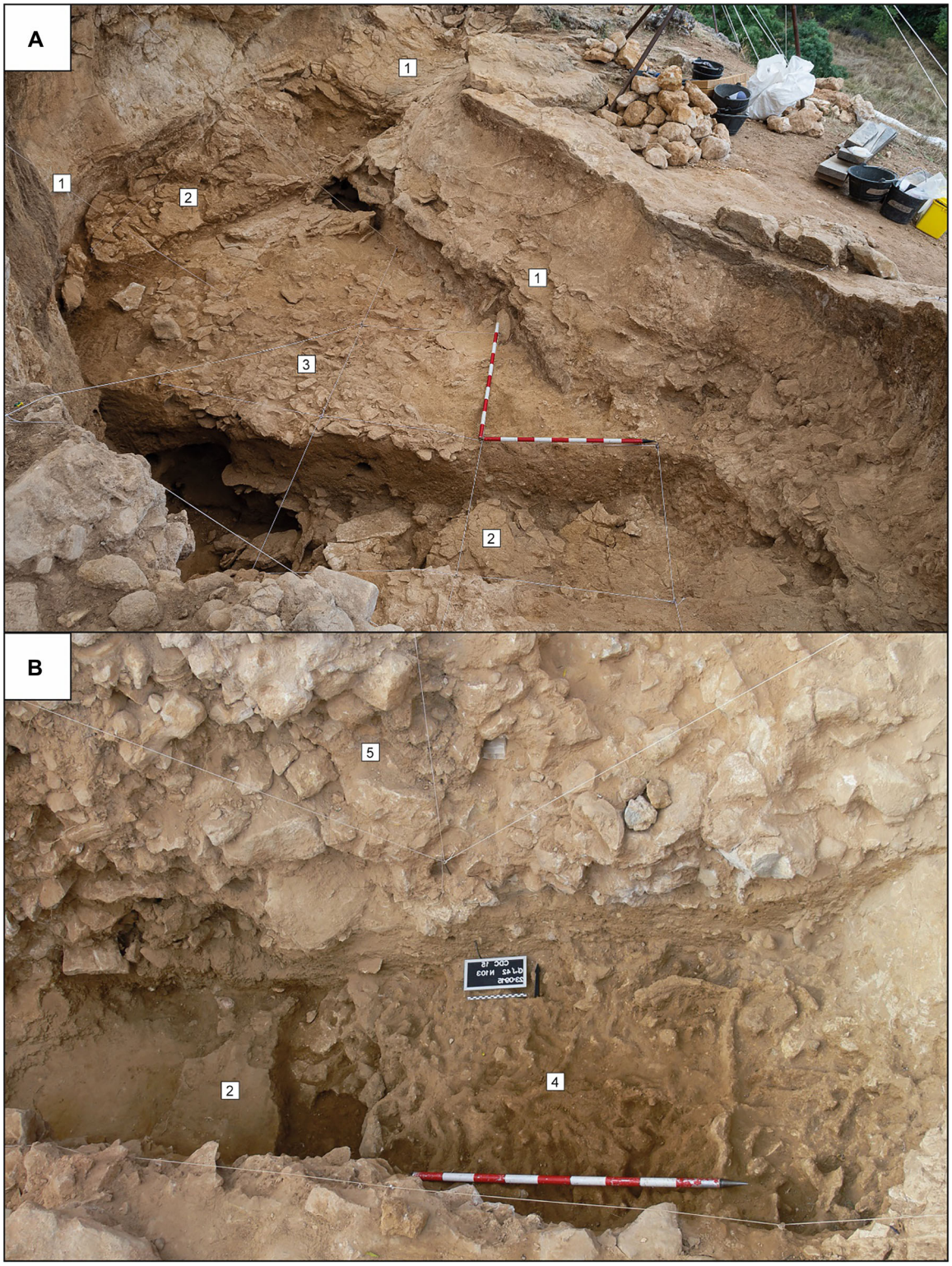

Figure 10. Photographs of Monumental Sector during different stages of excavation. (A) 2020 excavation campaign. (B) 2015 excavation campaign. 1: In situ S1 speleothem; 2: Fallen blocks of S1 speleothem in the contact between Units 7 and 6; 3: Unit 4 prismatic blocks; 4: Gour surface between Units 5 and 6; 5: Unit 3. [Color figure can be viewed at wileyonlinelibrary.com]

gravels are heterometric, containing rounded and subrounded limestone and dolostone pebbles and cobbles within an autochthonous silty sand matrix (Tables 1, 2, and 4). Unit 3.1 contains evidence of Neanderthal activity, including Mousterian lithic tools and hearths.

E3 speleothem: A thin (2 cm) flowstone conformably overlies Unit 3.1. It is found in situ close to the cave walls, but it has eroded elsewhere.

Unit H: The uppermost Unit H consists of a <10 cm thick dark brown (7.5YR 3/3) Ap soil horizon that disconformably overlies Units 1, 2 and 3.1. The soil horizon includes reworked fossil material from these underlying units. As in the Monumental Sector, another sink is found in the easternmost part of this sector.

Des-Cubierta karst evolution

The evolution of the Des-Cubierta karst system can be understood within the framework of classical speleogenetic stages: juvenile, mature, and senile phases (Llopis Lladó, 1970). These phases reflect the progressive development of the cave

© 2025 The Authors *Journal of Quaternary Science* Published by John Wiley & Sons Ltd.

10991417, 0, Downloaded from https://onlinelibrary.wiley.com/doi/10.1002/jqs.3722 by Universidad Complutense De, Wiley Online Library on [30/05/2025]. See the Terms and Conditions (https://onlinelibrary.wiley.com/terms-and-conditions) on Wiley Online Library for rules of use; OA articles are governed by the applicable Creative Commons License

Table 4. Quantitative analysis of major elements (X-ray fluorescence).

	SiO2	Al2O3	Fe2O3t	MnO	MgO	CaO	Na2O	K2O	TiO2	P2O5	SO3	LOI	TOTAL
Unit 1	11.38	3.19	1.01	0.02	7.1	37	0.17	0.57	0.14	1.46	-	37.95	99.99
Unit 1	13.11	3.78	1.34	0.02	8.5	33.4	0.18	0.66	0.17	0.16	-	38.64	99.96
Unit 2	7.29	2.15	0.71	-	6.59	41.43	0.12	0.37	0.09	0.29	-	40.92	99.96
Unit 3	30.65	6.14	1.51	0.03	8.46	22.53	0.42	1.69	0.23	0.15	-	28.19	100
Unit 3	20.33	4.31	1.18	0.02	6.28	32.06	0.27	1.06	0.17	0.47	-	33.82	99.97
Unit 3	16.69	4.69	1.72	0.04	14.88	23.95	0.19	0.82	0.22	0.17	-	36.61	99.98
Unit 3.1	17.25	5.39	1.89	0.05	10.89	27.68	0.19	0.9	0.27	0.94	-	34.53	99.98
Unit 3.1	15.72	4.24	1.23	0.02	3.24	38.55	0.2	0.83	0.16	0.49	-	35.3	99.98

LOI: Loss on ignition.

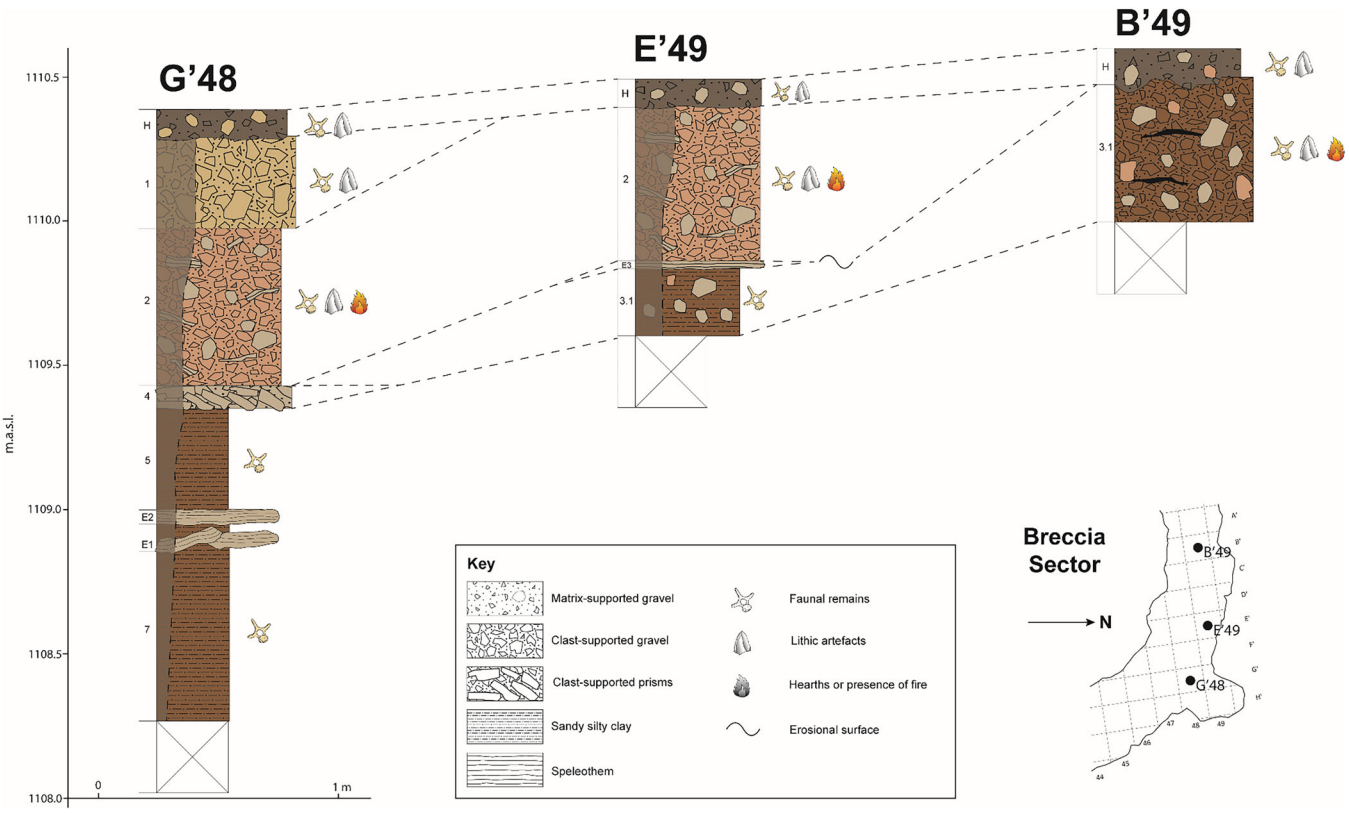

Figure 11. Detailed stratigraphic sections of Breccia Sector in Des-Cubierta Cave. [Color figure can be viewed at wileyonlinelibrary.com]

from its early formation through fluvial and speleothemic processes to its final stages dominated by roof and wall collapse and sediment infill. The stratigraphic units and corresponding facies preserved within the cave provide crucial insights into these evolutionary stages (Table 5).

During the juvenile phase, fluvial processes played a dominant role in sediment deposition. This phase is represented by Units 12–7, consisting of backswamp, slackwater and channel deposits. Given the interpreted age of Unit 10 (300–400 ka), this phase likely corresponds to MIS 11–10.

A brief, initial mature phase developed during MIS 7, marked by extensive speleothem precipitation (S1 speleothem). The widespread development of speleothems indicates a period of reduced sedimentation and stable hydrological conditions. One of the most significant consequences of this speleothem growth was the sealing of certain cave passages, effectively disconnecting the Cubil Sector from the Monumental Sector. This barrier would have influenced subsequent depositional environments and may have impacted the transit of large animals and Neanderthals.

However, this stable hydrological phase was abruptly interrupted, leading to a second juvenile phase, which likely occurred between the end of MIS7 and MIS5. This regression into a second juvenile phase is marked by significant erosive processes, which partially eroded the S1 speleothem and Unit 7. These erosional events were followed by the deposition of Units 6 and 5, which consisted of slackwater facies.

The main mature phase of the karst is characterised by stages of speleothem growth (S2 and E3 speleothems) interspersed with rockfall facies (Units 3 and 4). During MIS4, a collapse doline formed, marking the beginning of the cave's progressive opening. The transition from hydrologically driven sedimentation to gravitational collapse signifies the cave's shift from an active fluvial system to a progressively open setting, where external weathering and roof instability dominated sedimentation.

The senile phase represents the final stage of karst evolution, characterised by extensive collapse of the cave walls and the accumulation of rockfall deposits containing both autochthonous and allochthonous sediments. This phase is recorded in Units 2 and 1, which likely accumulated sometime during MIS 4 or 3. By this time, the cave had lost most of its roof, resulting in increased sedimentation of allochthonous wind-borne silts and sands within the dolostone breakdown clasts, suggesting that the cave had become an open system, with sediment infill and erosion marking the last phase of its geological evolution.

© 2025 The Authors *Journal of Quaternary Science* Published by John Wiley & Sons Ltd.

10991417, 0, Downloaded from https://onlinelibrary.wiley.com/doi/10.1002/jqs.3722 by Universidad Complutense De, Wiley Online Library on [30/05/2025]. See the Terms and Conditions (https://onlinelibrary.wiley.com/terms-and-conditions) on Wiley Online Library for rules of use; OA articles are governed by the applicable Creative Commons License

Table 5. Summary table of the main lithostratigraphic units identified in Des-Cubierta Cave, detailing their corresponding facies and estimated ages. The table also integrates the units into the broader framework of karst evolution.

Unit	Facies	Origin	Age	Karst Evolution
1	Rockfall	Autochthonous clasts, mixed matrix		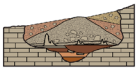 Senile phase
2	Rockfall	Autochthonous clasts, mixed matrix	MIS 4/3	
E3	Speleothem	-		 Mature phase
3	Rockfall	Autochthonous	MIS 4	
4	Rockfall	Autochthonous		
S2	Speleothem	-	MIS 6/5	
5	Slackwater	Allochthonous		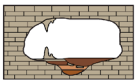 Juvenile phase
6	Slackwater	Allochthonous		
S1	Speleothem	-	MIS 7	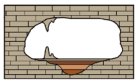 Mature phase
7	Slackwater	Allochthonous		Juvenile phase
8	Channel	Allochthonous		
9	Slackwater	Allochthonous		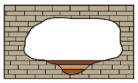
10	Channel	Allochthonous	MIS 11/10	
11	Backswamp	Autochthonous		
12	Backswamp	Autochthonous		
				(Embryonic phase)

Neanderthal cave entrances

The question of how Neanderthals entered Des-Cubierta Cave, particularly concerning the deposits in Unit 3, is a critical aspect of understanding their occupation and use of the space. One plausible entry point could have been the opening above the apex of Unit 3's debris cone. This opening, inferred from the sedimentology and geometry of the deposits, aligns with the contact between the Cretaceous upper and middle units, suggesting that the cave was open to the exterior during the rockfall episodes. However, this opening is situated approximately 2 m above the level of the debris cone, making it unlikely that Neanderthals would have easily descended or jumped such a distance, especially given the hazardous nature of the drop. The possibility that they later climbed back out also seems improbable, as it would require advanced climbing skills or tools not evidenced elsewhere in the archaeological record. While there is some minor evidence of fibre use among Neanderthals (Hardy et al., 2020), this remains insufficient to support the likelihood of their utilising such aids for climbing, thus reinforcing the improbability of this scenario.

A more likely scenario involves an alternative entrance. Towards the south of the Monumental Sector, a lower unit of Late Cretaceous marl is present, which is particularly erodible compared to the limestone and dolostone units above. As previously discussed, this marl layer has been subject to erosion for a prolonged period, dating back to MIS7, as evidenced by the extensive development of speleothems in that part of the cave. The intense erosion of this unit, driven by water flow over millennia, could have progressively weakened and widened the cave's southern boundary.

Around 50 000 years ago, as the cave began to open to the exterior more significantly, the erosion likely progressed not only vertically but also laterally, from the south to the north, towards the present-day river base level. This erosional process would have affected the more fragile marl layers first, potentially creating a side opening in the southern part of the cave, providing a more accessible entrance for Neanderthals. This southern opening would have been far less challenging to navigate than the 2-m drop associated with the collapsed doline opening, making it a more practical entry point.

Site formation history

The geological history of Des-Cubierta Cave (Fig. 12) records a complex sequence of depositional and erosional events spanning hundreds of thousands of years. The earliest deposits in the cave are represented by Units 12 to 7, primarily composed of fluvial sediments. Geomorphological correlations with terraces in the Madrid Basin, located at a similar elevation (~20 m above the thalweg), suggest that these units were deposited between 300 000 and 400 000 years ago. These deposits contain primarily faunal remains, including carnivorans and bats (Fig. 12B).

© 2025 The Authors *Journal of Quaternary Science* Published by John Wiley & Sons Ltd.

10991417, 0, Downloaded from https://onlinelibrary.wiley.com/doi/10.1002/jqs.3722 by Universidad Complutense De, Wiley Online Library on [30/05/2025]. See the Terms and Conditions (https://onlinelibrary.wiley.com/terms-and-conditions) on Wiley Online Library for rules of use; OA articles are governed by the applicable Creative Commons License

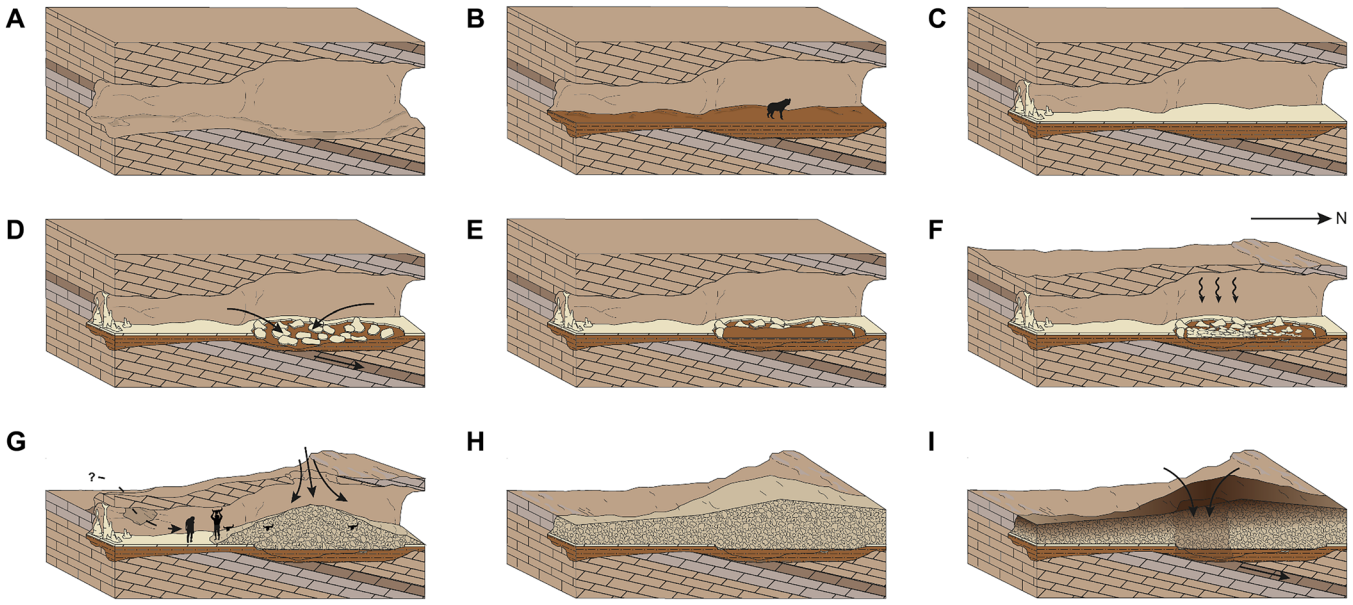

Figure 12. Site formation history. (A) Speleogenesis, heavily influenced by Late Cretaceous shoaling upwards sequences. (B) Fluvial deposition (Units 12 to 7) and denning activities. (C) Speleothem precipitation (S1). (D) Erosion and speleothem gravitational collapse. (E) Deposition of Units 5 and 6. (F) Deposition of Unit 4. (G) Deposition of Unit 3. First cave openings and Neanderthal occupation. (H) Erosion and denudation after cave infill. (I) Holocene soil development and active sinks. [Color figure can be viewed at wileyonlinelibrary.com]

During MIS 7, the cave experienced intense speleothem formation, most notably the development of the S1 speleothem (Fig. 12(C)). This flowstone was well developed between the Cubil and Monumental Sectors, likely due to the increased erosion of the Late Cretaceous marl units, allowing water to flow more freely through the cave. Over time, this extensive speleothem precipitation sealed the narrow passage between these two sectors.

Intense erosion partially removed the top of Unit 7 and led to the gravitational collapse of the S1 speleothem, particularly in the wider areas of the cave (Fig. 12(D)). Over the collapsed speleothem fragments, Unit 6, a sandy silty clay deposit, was laid down (Fig. 12(E)). This unit was later eroded, forming an eastward-dipping erosional surface, over which a microgour surface developed due to the partial cementation of clays. Then, Unit 5, composed of sandy and silty clay, was deposited.

The S2 speleothem precipitated over Unit 5. Associated with this speleothem were several stalagmites, one dated to 135.7 ± 1.9 ka, corresponding to MIS6a. The deposition of Unit 4 followed, consisting of flat, angular limestone and dolostone cobbles and boulders likely formed due to frost weathering of the cave walls and roof during cold periods (Fig. 12(F)).

Overlying Unit 4 is Unit 3, a gravel deposit representing the initial stages of the cave roof's collapse (Fig. 12(G)). This deposit comprises angular cobbles and boulders with a scant autochthonous carbonatic matrix, with little to no allochthonous input. This unit's pollen and micromammal assemblages (Baquedano et al., 2023, Supporting Information) suggest deposition during a cold period, likely MIS4. Neanderthal activity is well-documented within Unit 3, with Mousterian lithic tools and faunal remains, particularly large mammal crania. This unusual accumulation of cranial remains suggests Neanderthal symbolic behaviour. The sedimentological evidence suggests that this behaviour persisted over an extended period as depositional processes were prolonged and multiphasic.

Unit 3.1 was deposited sometime between the deposition of Units 4 and 2, although its relationship with Unit 3 is not yet fully understood. Unit 2, which lies conformably over Unit 3, contains rounded and subrounded pebbles and cobbles in a silty sand matrix. The presence of quartz, feldspar, mica, and igneous rock fragments in the matrix suggests that, by this time, openings had formed in the cave, allowing for allochthonous input. A charcoal fragment from this unit was dated to more than ~43 000 cal BP as described above. Pollen analyses (Baquedano et al., 2023, Supporting Information) further support that Unit 2 was deposited during a warm interstadial, consistent with the dating, placing it within MIS 3.

Unit 1, which conformably overlies Unit 2, marks a continuation of the denudation and erosion processes affecting the cave, with significant allochthonous material deposited during this phase (Fig. 12(H)). Level H, a Holocene soil horizon that unconformably overlies Units 1, 2, 3 and 3.1, represents the final sedimentation phase. Two sinks, located in the eastern parts of the Monumental and Breccia Sectors, are associated with the erosion of the Late Cretaceous marls and have affected the entire stratigraphic succession (Fig. 12(I)).

Conclusions

The complex geological history of Des-Cubierta Cave reflects a dynamic interplay of speleogenesis, fluvial processes, speleothem formation, erosional events, gravitational processes and Neanderthal occupations, represented in 12 lithostratigraphic units.

The earliest deposits, represented by Units 12 to 7, are fluvial sediments correlated with Middle Pleistocene terraces of the Lozoya River, suggesting a deposition age of 300 000–400 000 years ago.

Significant speleothem formation occurred during MIS 9 through 7, most notably the S1 speleothem, which sealed passages between cave sectors. A subsequent interglacial–glacial transition led to the erosion of Unit 7 and the collapse of the S1 speleothem, followed by the deposition of Units 6 and 5. Later, during MIS 6a, the S2 speleothem formed, and frost weathering contributed to the deposition of Unit 4.

Unit 3 hosts an unusual assemblage of large mammal cranial remains, interpreted as a symbolic practice. This unit was deposited during cold periods (likely MIS 4) and formed over multiple rockfall episodes. Its prolonged and multiphase deposition would suggest that the Neanderthal symbolic

© 2025 The Authors *Journal of Quaternary Science* Published by John Wiley & Sons Ltd.

10991417, 0, Downloaded from https://onlinelibrary.wiley.com/doi/10.1002/jqs.3722 by Universidad Complutense De, Wiley Online Library on [30/05/2025]. See the Terms and Conditions (https://onlinelibrary.wiley.com/terms-and-conditions) on Wiley Online Library for rules of use; OA articles are governed by the applicable Creative Commons License

practices were not isolated incidents but behaviours maintained and transmitted across multiple generations.

Acknowledgements. This research was funded by the Dirección General de Investigación e Innovación Tecnológica de la Comunidad de Madrid, grant no. H2019/HUM-5840 (co-financed by the European Social Fund), and by the Agencia Estatal de Investigación of the Ministerio de Ciencia, Innovación y Universidades, grant no. PCG2018-094125-B-100 (MCIU/AEI/FEDER, EU). D.M.M.P. is the recipient of a Margarita Salas postdoctoral grant funded by the Complutense University of Madrid (POP-UCM-CT18/22). AM is funded by a postdoctoral grant from the Fyssen Foundation.

Consent

During the preparation of this work, the authors used Grammarly and OpenAI ChatGPT with caution in order to improve language and readability. After using these tools/services, the authors reviewed and edited the content as needed and take full responsibility for the content of the publication.

Data availability statement

Data that support the findings of this study are available from the corresponding author upon reasonable request.

Supporting information

Additional supporting information can be found in the online version of this article.

Supmat.docx.

References

Abrunhosa, A., Bustillo, M.Á., Pereira, T., Márquez, B., Pérez-González, A., Arsuaga, J.L. et al. (2020) Petrographic and SEM-EDX characterization of Mousterian white/beige chert tools from the Navalmaíllo rock shelter (Madrid, Spain). *Geoarchaeology*, 35, 883–896. Available from: https://doi.org/10.1002/gea.21811

Abrunhosa, A., Márquez, B., Baquedano, E., Bicho, N., Pérez-González, A. & Arsuaga, J.L. (2014) Raw material study of the Mousterian lithic assemblage of Navalmaíllo rockshelter (Pinilla del Valle, Spain): preliminary results. *Estudos do Quaternário. Revista da Associacao Portuguesa para o Estudo do Quaternario*, 11, 19–25.

Abrunhosa, A., Pereira, T., Márquez, B., Baquedano, E., Arsuaga, J.L. & Pérez-González, A. (2019) Understanding Neanderthal technological adaptation at Navalmaíllo Rock Shelter (Spain) by measuring lithic raw materials performance variability. *Archaeological and Anthropological Sciences*, 11, 5949–5962. Available from: https://doi.org/10.1007/s12520-019-00826-3

Aldeias, V., Sandgathe, D., McPherron, S.J.P., Bruxelles, L., Turq, A. & Goldberg, P. (2023) Site formation histories and context of human occupations at the Paleolithic site of La Ferrassie (Dordogne, France). *Journal of Paleolithic Archaeology*, 6, 30. Available from: https://doi.org/10.1007/s41982-023-00159-7

Alférez, F., Brea, P., Buitrago, A.M., Bustos, V., Molero, G. & Delgado, F.A. (1982) Descubrimiento del primer yacimiento cuaternario (Riss-Würm) de vertebrados con restos humanos en la provincia de Madrid (Pinilla del Valle). *Coloquios de Paleontología*, 37, 15–32. Available from: https://revistas.ucm.es/index.php/COPA/article/view/COPA8282110015A

Álvarez-Alonso, D., de Andrés-Herrero, M., Díez-Herrero, A., Rojo Hernández, J.A. (2018) Análisis geoarqueológico de las ocupaciones musterienses en el valle alto del río Eresma: el Abrigo del Molino (Segovia, España). *Boletín Geológico y Minero*, 129(1/2), 153–182.

Álvarez-Lao, D.J., Arsuaga, J.L., Baquedano, E. & Pérez-González, A. (2013) Last Interglacial (MIS 5) ungulate assemblage from the Central Iberian Peninsula: the Camino Cave (Pinilla del Valle, Madrid, Spain). *Palaeogeography, Palaeoclimatology, Palaeoecology*, 374, 327–337. Available from: https://doi.org/10.1016/j.palaeo.2013.01.025

Angelucci, D.E., Nabais, M. & Zilhão, J. (2023) Formation processes, fire use, and patterns of human occupation across the Middle Palaeolithic (MIS 5a-5b) of Gruta da Oliveira (Almonda karst system, Torres Novas, Portugal). *PLoS One*, 18(10), e0292075.

Angelucci, D.E., Zambaldi, M., Tessari, U., Vaccaro, C., Arnaud, J., Berruti, G.L.F. et al. (2018) New insights on the Monte Fenera Palaeolithic, Italy: geoarchaeology of the Ciota Ciara cave. *Geoarchaeology*, 34(4), 413–429.

Aranburu, A., Arsuaga, J.L. & Sala, N. (2017) The stratigraphy of the Sima de los Huesos (Atapuerca, Spain) and implications for the origin of the fossil hominin accumulation. *Quaternary International*, 433, 5–21.

Arenas-Martín, R., Fuster, J.M., Martínez, J., Del Olmo, A. & Villaseca, E. (1991) *Mapa Geológico de España a E. 1:50.000, Segovia (483)*. Madrid, España: Instituto Geológico y Minero de España (IGME).

Arriaza, M.C., Huguet, R., Laplana, C., Pérez-González, A., Márquez, B., Arsuaga, J.L. et al. (2017) Lagomorph predation represented in a middle Palaeolithic level of the Navalmaíllo Rock Shelter site (Pinilla del Valle, Spain), as inferred via a new use of classical taphonomic criteria. *Quaternary International*, 436, 294–306. Available from: https://doi.org/10.1016/j.quaint.2015.03.040

Arriolabengoa, M., Iriarte, E., Aranburu, A., Yusta, I., Arnold, L.J., Demuro, M. et al. (2018) Reconstructing the sedimentary history of Lezetxiki II cave (Basque Country, northern Iberian Peninsula) using micromorphological analysis. *Sedimentary Geology*, 372, 96–111.

Arsuaga, J.L., Baquedano, E. & Pérez-González, A. (2011) Neanderthal and carnivore occupations in Pinilla del Valle sites (Community of Madrid, Spain). In: Oosterbeek, L. & Fidalgo, C. (Eds.) *Proceedings of the XV World Congress of the International Union for Prehistoric and Protohistoric Sciences*. England: Archeopress, pp. 111–119.

Arsuaga, J.L., Baquedano, E., Pérez-González, A., Sala, N., García, García, N. et al. (2010) El yacimiento arqueopaleontológico del Pleistoceno Superior de la Cueva del Camino en el Calvero de la Higuera (Pinilla del Valle, Madrid). *Zona Arqueológica*, 13, 421–442.

Arsuaga, J.L., Baquedano, E., Pérez-González, A., Sala, N., Quam, R.M., Rodríguez, L. et al. (2012) Understanding the ancient habitats of the last-interglacial (late MIS 5) Neanderthals of central Iberia: paleoenvironmental and taphonomic evidence from the Cueva del Camino (Spain) site. *Quaternary International*, 275, 55–75. Available from: https://doi.org/10.1016/j.quaint.2012.04.019

Auler, A.S., Smart, P.L., Wang, X., Piló, L.B., Edwards, R.L. & Cheng, H. (2009) Cyclic sedimentation in Brazilian caves: mechanisms and palaeoenvironmental significance. *Geomorphology*, 106, 142–153.

Balzeau, A., Turq, A., Talamo, S., Daujeard, C., Guérin, G., Welker, F. et al. (2020) Pluridisciplinary evidence for burial for the La Ferrassie 8 Neandertal child. *Scientific Reports*, 10, 21230. Available from: https://doi.org/10.1038/s41598-020-77611-z.

Baquedano, E., Arsuaga, J.L. & Pérez-González, A. (2010) Homínidos y carnívoros: competencias en un mismo nicho ecológico pleistoceno: los yacimientos del Calvero de la Higuera en Pinilla del Valle. *Actas de las Quintas Jornadas de Patrimonio Arqueológico en la Comunidad de Madrid*, 1, 61–72.

Baquedano, E., Arsuaga, J.L., Pérez-González, A., Laplana, C., Márquez, B., Huguet, R. et al. (2023) A symbolic Neanderthal accumulation of large herbivore crania. *Nature Human Behaviour*, 7, 342–352. Available from: https://doi.org/10.1038/s41562-022-01503-7

Baquedano, E., Arsuaga, J.L., Pérez-González, A., Márquez, B., Laplana, C., Ortega Martínez, M.C. et al. (2016) The Des-Cubierta Cave (Pinilla del Valle, Comunidad de Madrid, Spain): a Neanderthal site with a likely funerary/realistic connection. Presented at 6th Annual European Society for the study of Human Evolution Meeting, Alcalá de Henares.

Baquedano, E., Márquez, B., Laplana, C., Arsuaga, J.L. & Pérez-González, A. (2014) The archaeological sites at Pinilla del Valle (Madrid, Spain). In: Sala, R., (ed) *Pleistocene and Holocene hunter-gatherers in Iberia and the Gibraltar strait: the current archaeological record*. Burgos: Fundación Atapuerca. pp. 577–584.

Baquedano, E., Márquez, B., Pérez-González, A., Mosquera, M., Huguet, R., Espinosa, J.A. et al. (2012) Neandertales en el valle del Lozoya: los yacimientos paleolíticos del Calvero de la Higuera (Pinilla del Valle, Madrid). *Mainake*, 33, 83–100.

Bellido, F., Escuder, J., Klein, E. & Del Olmo, A. (1991) *Mapa Geológico de España a E. 1:50.000, Buitrago de Lozoya (484)*. Madrid, España.: Instituto Geológico y Minero de España (IGME).

© 2025 The Authors *Journal of Quaternary Science* Published by John Wiley & Sons Ltd.

10991417, 0, Downloaded from https://onlinelibrary.wiley.com/doi/10.1002/jqs.3722 by Universidad Complutense De, Wiley Online Library on [30/05/2025]. See the Terms and Conditions (https://onlinelibrary.wiley.com/terms-and-conditions) on Wiley Online Library for rules of use; OA articles are governed by the applicable Creative Commons License

Bello, S.M. (2021) Boning up on Neanderthal art. *Nature Ecology & Evolution*, 5, 1201–1202. Available from: https://doi.org/10.1038/s41559-021-01506-z

Blain, H.A., Laplana, C., Sánchez-Bandera, C., Fagoaga, A., Blanco Lapaz, Á., Martínez-Monzón, A. et al. (2022) A warm and humid paleoecological context for the Neanderthal mountain settlement at the Navalmaíllo rockshelter (Iberian Central System, Madrid). *Quaternary Science Reviews*, 293, 107727. Available from: https://doi.org/10.1016/j.quascirev.2022.107727.

Blain, H.A., Laplana, C., Sevilla, P., Arsuaga, J.L., Baquedano, E. & Pérez-González, A. (2014) MIS 5/4 transition in a mountain environment: herpetofaunal assemblages from Cueva del Camino, central Spain. *Boreas*, 43, 107–120. Available from: https://doi.org/10.1111/bor.12024

Blott, S.J. & Pye, K. (2012) Particle size scales and classification of sediment types based on particle size distributions: review and recommended procedures. *Sedimentology*, 59(7), 2071–2096. Available from: https://doi.org/10.1111/j.1365-3091.2012.01335.x

Bosch, R.F. & White, W.B. (2018) Lithofacies and transport of clastic sediments in karst conduits. In: White, W., Herman, J., Herman, E. & Rutigliano, M., eds. *Karst Groundwater Contamination and Public Health. Advance in Karst Science*. Cham: Springer. pp. 277–281. https://doi.org/10.1007/978-3-319-51070-5_32

Bull, P.A. (1981) Some fine-grained sedimentation phenomena in caves. *Earth Surface Processes & Landforms*, 6(1), 11–22.

Campaña, I., Benito-Calvo, A., Pérez-González, A., Álvaro-Gallo, A., Miguens-Rodríguez, L., Iglesias-Cibanal, J. et al. (2022) Revision of TD1 and TD2 stratigraphic sequence of Gran Dolina cave (Sierra de Atapuerca, Spain). *Journal of Iberian Geology*, 48, 425–443.

Campaña, I., Benito-Calvo, A., Pérez-González, A., Ortega, A.I., Bermúdez de Castro, J.M. & Carbonell, E. (2017) Pleistocene sedimentary facies of the Gran Dolina archaeo-paleoanthropological site (Sierra de Atapuerca, Burgos, Spain). *Quaternary International*, 433(A), 68–84.

Chung, F.H. (1975) Quantitative interpretation of X-ray diffraction patterns of mixtures. III. Simultaneous determination of a set of reference intensities. *Journal of Applied Crystallography*, 8(1), 17–19. Available from: https://doi.org/10.1107/S0021889875009454

Frayer, D. (2019) Neanderthals and the black swan. *Paleoanthropology*, 2019, 350–361. Available from: https://doi.org/10.4207/PA.2019.ART135

Frayer, D.W., Radovčić, J. & Radovčić, D. (2020) Krapina and the case for Neandertal symbolic behavior. *Current Anthropology*, 61(6), 713–731. Available from: https://doi.org/10.1086/712088

Galindo-Pellicena, M.A., Arsuaga, J.L., Laplana, C., de Gaspar, I., Álvarez-Lao, D., Pérez-González, A. et al. (2019) Distinguishing between *Bos* and *Bison* petrous bones. A case study: bovines from the Des-Cubierta Cave (Pinilla del Valle, Madrid). *Spanish Journal of Palaeontology*, 34(2), 257–268. Available from: https://doi.org/10.7203/sjp.34.2.16115

Gillieson, D. (1996) *Caves: processes, development and management*. Oxford: Blackwell.

Goldberg, P. (2000) Micromorphology and site formation at Die Kelders cave I, South Africa. *Journal of Human Evolution*, 38(1), 43–90.

Goldberg, P. & Bar-Yosef, O. (1998) Site formation processes in Kebara and Hayonim caves and their significance in Levantine prehistoric caves, In: *Neandertals and modern humans in Western Asia*. Springer US. pp. 107–125.

Goldberg, P. & Berna, F. (2010) Micromorphology and context. *Quaternary International*, 214(1–2), 56–62.

Goldberg, P. & Sherwood, S.C. (2006) Deciphering human prehistory through the geoarcheological study of cave sediments. *Evolutionary Anthropology: Issues, News, and Reviews*, 15(1), 20–36.

Goldberg, P., Weiner, S., Bar-Yosef, O., Xu, Q. & Liu, J. (2001) Site formation processes at Zhoukoudian, China. *Journal of Human Evolution*, 41(5), 483–530.

Hardy, B.L., Moncel, M.H., Kerfant, C., Lebon, M., Bellot-Gurlet, L. & Mélard, N. (2020) Direct evidence of Neanderthal fibre technology and its cognitive and behavioral implications. *Scientific Reports*, 10, 4889. Available from: https://doi.org/10.1038/s41598-020-61839-w

Herman, E.K., Toran, L. & White, W.B. (2012) Clastic sediment transport and storage in fluviokarst aquifers: an essential component of karst hydrogeology. *Carbonates and Evaporites*, 27, 211–241.

Hoffmann, D.L., Standish, C.D., García-Diez, M., Pettitt, P.B., Milton, J.A., Zilhão, J. et al. (2018) U-Th dating of carbonate crusts reveals Neandertal origin of Iberian cave art. *Science*, 359(6378), 912–915. Available from: https://doi.org/10.1126/science.aap7778

Huguet, R., Arsuaga, J.L., Pérez-González, A., Arriaza, M.C., Sala, N., Laplana, C. et al. (2010) Homínidos y hienas en el Calvero de la Higuera (Pinilla del Valle, Madrid) durante el Pleistoceno Superior. Resultados preliminares. *Zona Arqueológica*, 13, 443–458.

Iacoviello, F. & Martini, I. (2012) Provenance and geological significance of red mud and other clastic sediments of the Mugnano Cave (Montagnola Senese, Italy). *International Journal of Speleology*, 41(2), 317–328. https://doi.org/10.5038/1827-806X.41.2.17

Jaubert, J., Verheyden, S., Genty, D., Soulier, M., Cheng, H., Blamart, D. et al. (2016) Early Neanderthal constructions deep in Bruniquel Cave in southwestern France. *Nature*, 534, 111–114. Available from: https://doi.org/10.1038/nature18291

Jimenez, I.J., Laplana, C., García-Real, M.I., Baquedano, E., Arsuaga, J.L. & Garcia, N. (2024) "Society of the den": identifying patterns of denning behaviour in Upper Pleistocene hyena populations. *Quaternary Science Reviews*, 345, 109004. Available from: https://doi.org/10.1016/j.quascirev.2024.109004

Karampaglidis, T. (2014) La evolución geomorfológica de la cuenca de drenaje del río Lozoya (Comunidad de Madrid, España). PhD Thesis. Complutense University of Madrid. Madrid, Spain. https://hdl.handle.net/20.500.14352/26147

Karkanas, P. (2001) Site formation processes in Theopetra Cave: a record of climatic change during the Late Pleistocene and Early Holocene in Thessaly, Greece. *Geoarchaeology*, 16(4), 373–399.

Karkanas, P. & Goldberg, P. (2010) Site formation processes at Pinnacle point cave 13B (Mossel Bay, Western Cape Province, South Africa): resolving stratigraphic and depositional complexities with micromorphology. *Journal of Human Evolution*, 59, 256–273.

Laborda-López, C., Martín-Perea, D.M., Del Castillo, E., Alías Linares, M.A., Iannicelli, C., Pal, S. et al. (2024) Sedimentological evolution of the Quibas site: high-resolution glacial/interglacial dynamics in a terrestrial pre-Jaramillo to post-Jaramillo sequence from southern Iberian Peninsula. *Quaternary International*, 692, 28–44.

Laplana, C. & Sevilla, P. (2006) Nuevos datos sobre los micromamíferos (Roedores, Insectívoros y Quirópteros) del yacimiento Camino (Pleistoceno Superior, Pinilla del Valle, Madrid). In: Fernández-Martínez E. (Ed.) *Libro de Resúmenes de las XXII Jornadas de Paleontología*, Sociedad Española de Paleontologia, pp. 135–137.

Laplana, C., Blain, H.A., Sevilla, P., Arsuaga, J.L., Baquedano, E. & Pérez-González, A. (2013) Un assemblage de petits vertébrés hautement diversifié de la fin du MIS 5 dans un environnement montagnard au Centre de l'Espagne (Cueva del Camino, Pinilla del Valle, communauté autonome de Madrid). *Quaternaire*, 24(2), 207–216. Available from: https://doi.org/10.4000/quaternaire.6617

Laplana, C., Sevilla, P., Arsuaga, J.L., Arriaza, M.C., Baquedano, E., Pérez-González, A. et al. (2015) How far into Europe did pikas (Lagomorpha: Ochotonidae) go during the Pleistocene? New evidence from Central Iberia. *PLoS One*, 10, e0140513. Available from: https://doi.org/10.1371/journal.pone.0140513

Laplana, C., Sevilla, P., Blain, H.A., Arriaza, M.C., Arsuaga, J.L., Pérez-González, A. et al. (2016) Cold-climate rodent indicators for the Late Pleistocene of Central Iberia: new data from the Buena Pinta Cave (Pinilla del Valle, Madrid Region, Spain). *Comptes Rendus Palevol*, 15, 696–706. Available from: https://doi.org/10.1016/j.crpv.2015.05.010

Laureano, F.V., Karmann, I., Granger, D.E., Auler, A.S., Almeida, R.P., Cruz, F.W. et al. (2016) Two million years of river and cave aggradation in NE Brazil: implications for speleogenesis and landscape evolution. *Geomorphology*, 273, 63–77. Available from: https://doi.org/10.1016/j.geomorph.2016.08.009

Leder, D., Hermann, R., Hüls, M., Russo, G., Hoelzmann, P., Nielbock, R. et al. (2021) A 51,000-year-old engraved bone reveals Neanderthals' capacity for symbolic behaviour. *Nature Ecology & Evolution*, 5, 1273–1282. Available from: https://doi.org/10.1038/s41559-021-01487-z

Llopis Lladó, N. (1970). *Fundamentos de hidrogeologia carstica: introduccion a la geoespeleología*. Madrid: Blume, p. 629.

© 2025 The Authors *Journal of Quaternary Science* Published by John Wiley & Sons Ltd.

10991417, 0, Downloaded from https://onlinelibrary.wiley.com/doi/10.1002/jqs.3722 by Universidad Complutense De, Wiley Online Library on [30/05/2025]. See the Terms and Conditions (https://onlinelibrary.wiley.com/terms-and-conditions) on Wiley Online Library for rules of use; OA articles are governed by the applicable Creative Commons License

Majkić, A., d'Errico, F. & Stepanchuk, V. (2018) Assessing the significance of Palaeolithic engraved cortexes: a case study from the Mousterian site of Kiik-Koba, Crimea. *PLoS One*, 13(5), e0195049. Available from: https://doi.org/10.1371/journal.pone.0195049

Marean, C.W., Bar-Matthews, M., Fisher, E., Goldberg, P., Herries, A., Karkanas, P. et al. (2010) The stratigraphy of the middle stone age sediments at pinnacle point cave 13B (Mossel Bay, western Cape province, South Africa). *Journal of Human Evolution*, 59(3–4), 234–255.

Marquet, J.C., Freiesleben, T.H., Thomsen, K.J., Murray, A.S., Calligaro, M., Macaire, J.J. et al. (2023) The earliest unambiguous Neanderthal engravings on cave walls: La Roche-Cotard, Loire Valley, France. *PLoS One*, 18(6), e0286568. Available from: https://doi.org/10.1371/journal.pone.0286568

Márquez, B., Baquedano, E., Pérez-González, A. & Arsuaga, J.L. (2016b) Microwear analysis of Mousterian quartz tools from the Navalmaíllo Rock Shelter (Pinilla del Valle, Madrid, Spain). *Quaternary International*, 424, 84–97. Available from: https://doi.org/10.1016/j.quaint.2015.08.052

Márqueza, B., Baquedano, E., Pérez-González, A. & Arsuaga, J.L. (2017) Denticulados y muescas: ¿para qué sirven? Estudio funcional de una muestra musteriense en cuarzo del Abrigo de Navalmaíllo (Pinilla del Valle, Madrid, España). *Trabajos de Prehistoria*, 74(1), 26–46. Available from: https://doi.org/10.3989/tp.2017.12182

Márquez, B., Baquedano, E., Pérez-González, A., Laplana, C., Huguet, R., García, N. et al. (2016a) El Abrigo de Navalmaíllo (Pinilla del Valle, Madrid, España). Un campamento de Neandertales en el centro de la Península Ibérica. Alcalá de Henares.

Márquez, B., Mosquera, M., Pérez-González, A., Arsuaga, J.L., Baquedano, E., Panera, J. et al. (2013) Evidence of a neanderthal-made quartz-based technology at Navalmaíllo rockshelter (Pinilla del Valle, Madrid Region, Spain). *Journal of Anthropological Research*, 69, 373–395. Available from: https://doi.org/10.3998/jar.0521004.0069.306

Martini, I. (2011) Cave clastic sediments and implications for speleogenesis: new insights from the Mugnano Cave (Montagnola Senese, Northern Apennines, Italy). *Geomorphology*, 134(3–4), 452–460.

Martini, I., Baucon, A. & Boschin, F. (2021) Depositional processes and environmental settings in rock shelters: The case of the prehistoric Oscurusciuto site (Southern Italy). *Geological Magazine*, 158, 891–904.

Martini, I., Ronchitelli, A., Arrighi, S., Capecchi, G., Ricci, S., Scaramucci, S. et al. (2018) Cave clastic sediments as a tool for refining the study of human occupation of prehistoric sites: insights from the cave site of La Cala (Cilento, southern Italy). *Journal of Quaternary Science*, 33(5), 586–596.

Martín-Perea, D.M., Maíllo-Fernández, J.M., Marín, J., Arroyo, X. & Asiaín, R. (2022) A step back to move forward: a geological re-evaluation of the El Castillo Cave Middle Palaeolithic lithostratigraphic units (Cantabria, northern Iberia). *Journal of Quaternary Science*, 38(2), 221–234.

Mielgo, C., Huguet, R., Laplana, C., Martín-Perea, D.M., Moclán, A. & Márquez, B. et al. (2024) Intra-site spatial approaches based on taphonomic análisis to characterize the assemblage formation: a case study from Buena Pinta cave (Pinilla del Valle, Spain). *Archaeological and anthropological Science*, 16(1), 5. Available from: https://doi.org/10.1007/s12520-023-01913-2

Moclán, A., Domínguez-Rodrigo, M., Huguet, R., Pizarro-Monzo, M., Arsuaga, J.L. & Pérez-González, A. et al. (2024) Deep learning identification of anthropogenic modifications on a carnivore remain suggests use of hyena pelts by Neanderthals in the Navalmaíllo rock shelter (Pinilla del Valle, Spain). *Quaternary Science Reviews*, 329, 108560. https://doi.org/10.1016/j.quascirev.2024.10856

Moclán, A., Huguet, R., Márquez, B., Domínguez-Rodrigo, M., Gómez-Miguelsanz, C., Vergès, J.M. et al. (2018) Cut marks made with quartz tools: an experimental framework for understanding cut mark morphology, and its use at the Middle Palaeolithic site of the Navalmaíllo Rock Shelter (Pinilla del Valle, Madrid, Spain). *Quaternary International*, 493, 1–18. Available from: https://doi.org/10.1016/j.quaint.2018.09.033

Moclán, A., Huguet, R., Márquez, B., Laplana, C., Arsuaga, J.L., Pérez-González, A. et al. (2020) Identifying the bone-breaker at the Navalmaíllo Rock Shelter (Pinilla del Valle, Madrid) using machine learning algorithms. *Archaeological and Anthropological Sciences*, 12, 46. Available from: https://doi.org/10.1007/s12520-020-01017-1

Moclán, A., Huguet, R., Márquez, B., Laplana, C., Galindo-Pellicena, M.Á., García, N. et al. (2021) A neanderthal hunting camp in the central system of the Iberian Peninsula: a zooarchaeological and taphonomic analysis of the Navalmaíllo Rock Shelter (Pinilla del Valle, Spain). *Quaternary Science Reviews*, 269, 107142. Available from: https://doi.org/10.1016/j.quascirev.2021.107142

Munsell, A.H. (1981) *A Color Notation: an illustrated system defining all colors and their relations by measured scales for hue, value and chroma*, 14th edition. Baltimore: Munsell Color.

Nowell, A. & Cooke, A. (2021) Culturing the paleolithic body: archaeological signatures of adornment and body modification. In: Gontier, N., Lock, A. & Sinha, C. *Oxford handbook of human symbolic evolution*. Oxford, UK: Oxford University Press. https://doi.org/10.1093/oxfordhb/9780198813781.013.20

Panera, J., Torres, T., Pérez-González, A., Ortiz, J.E., Rubio-Jara, S. & Uribelarrea del Val, D. (2011) Geocronología de la Terraza Compleja de Arganda en el valle del río Jarama (Madrid, España). *Estudios Geológicos*, 67(2), 495–504.

Pérez-González, A., Arsuaga, J.L., Baquedano, E., Márquez, B., Karampaglidis, T. & Bárez, S. (2008) Neanderthal occupations in a rock-shelter and caves during the Late Pleistocene in Pinilla del Valle karst (Madrid, Spain). 13th Belgium-France-Italy-Romania Geomorphological Meeting. Landscape Evolution & Geoarchaeology.

Pérez-González, A., Karampaglidis, T., Arsuaga, J.L., Baquedano, E., Bárez, S., Gómez, J.J. et al. (2010) Aproximación geomorfológica a los yacimientos del Pleistoceno Superior del Calvero de la Higuera en el Valle Alto del Lozoya (Sistema Central Español, Madrid). *Zona Arqueológica*, 13, 403–420.

Pitarch Martí, A., Zilhão, J., d'Errico, F., Cantalejo-Duarte, P., Domínguez-Bella, S., Fullola, J.M. et al. (2021) The symbolic role of the underground world among Middle Paleolithic Neanderthals. *Proceedings of the National Academy of Sciences*, 118(33), e20211495118. Available from: https://doi.org/10.1073/pnas.2021495118.

Radovčić, D., Sršen, A.O., Radovčić, J. & Frayer, D.W. (2015) Evidence for Neandertal jewelry: modified white-tailed eagle claws at Krapina. *PLoS One*, 10(3), e0119802. Available from: https://doi.org/10.1371/journal.pone.0119802

Ramos-Muñoz, J., Cantalejo, P., Blumenröther, J., Bolin, V., Otto, T., Rotgänger, M. et al. (2022) The nature and chronology of human occupation at the Galerías Bajas, from Cueva de Ardales, Malaga, Spain. *PLoS One*, 17(6), e0266788. Available from: https://doi.org/10.1371/journal.pone.0266788

Rendu, W., Beauval, C., Crevecoeur, I., Bayle, P., Balzeau, A., Bismuth, T. et al. (2014) Evidence supporting an intentional Neandertal burial at La Chapelle-aux-Saints. *Proceedings of the National Academy of Sciences*, 111, 81–86. Available from: https://doi.org/10.1073/pnas.1316780110

Rodríguez-Hidalgo, A., Morales, J.I., Cebrià, A., Courtenay, L.A., Fernández-Marchena, J.L., García-Argudo, G. et al. (2019) The Châtelperronian Neanderthals of Cova Foradada (Calafell, Spain) used imperial eagle phalanges for symbolic purposes. *Science Advances*, 5(11), eaax1984. Available from: https://doi.org/10.1126/sciadv.aax1984

Rodríguez-Vidal, J., d'Errico, F., Pacheco, F.G., Blasco, R., Rosell, J., Jennings, R.P. et al. (2014) A rock engraving made by Neanderthals in Gibraltar. *Proceedings of the National Academy of Sciences*, 111(37), 13301–13306. Available from: https://doi.org/10.1073/pnas.1411529111

Silva, P.G., Roquero, E., López-Recio, M., Huerta, P. & Martínez-Graña, A.M. (2017) Chronology of fluvial terrace sequences for large Atlantic rivers in the Iberian Peninsula (Upper Tagus and Duero drainage basins, Central Spain). *Quaternary Science Reviews*, 166, 188–203. Available from: https://doi.org/10.1016/j.quascirev.2016.05.027

Springer, G.S. & Kite, J.S. (1997) River-derived slackwater sediments in caves along Cheat River, West Virginia. *Geomorphology*, 18, 91–100.

Vera, J.A. (Ed.) (2004) *Geología de España*. Madrid, España: Sociedad Geológica Española – Instituto Geológico y Minero de España (IGME).

De Vicente, G., Vegas, R., Muñoz Martín, A., Silva, P.G., Andriessen, P., Cloetingh, S. et al. (2007) Cenozoic thick-skinned deformation and topography evolution of the Spanish Central System. *Global and*

© 2025 The Authors *Journal of Quaternary Science* Published by John Wiley & Sons Ltd.

10991417, 0, Downloaded from https://onlinelibrary.wiley.com/doi/10.1002/jqs.3722 by Universidad Complutense De, Wiley Online Library on [30/05/2025]. See the Terms and Conditions (https://onlinelibrary.wiley.com/terms-and-conditions) on Wiley Online Library for rules of use; OA articles are governed by the applicable Creative Commons License

Planetary Change, 58, 335–381. Available from: https://doi.org/10.1016/j.gloplacha.2006.11.042

Warburton, J. & Álvarez, C. (1989) A thrust tectonic interpretation of the Guadarrama Mountains, Spanish Central System. In: Cámara Rupelo, P. (Ed.) *Libro Homenaje a Rafael Soler*. Madrid: Asociación de Geólogos y Geofísicos Españoles del Petróleo (AGGEP), pp. 147–155.

White, W.B. (2007) Cave sediments and paleoclimate. *Journal of Cave and Karst Studies*, 69(1), 76–93.

Zilhao, J. (2015) Lower and middle palaeolithic mortuary behaviours and the origins of ritual burial. In: Renfrew, C., Boyd, M.J. & Morley, I. (Eds.) *Death rituals, social order and the archaeology of immortality in the ancient world: death shall have no dominion*. New York: Cambridge University Press, pp. 27–44.

© 2025 The Authors *Journal of Quaternary Science* Published by John Wiley & Sons Ltd.

10991417, 0, Downloaded from https://onlinelibrary.wiley.com/doi/10.1002/jqs.3722 by Universidad Complutense De, Wiley Online Library on [30/05/2025]. See the Terms and Conditions (https://onlinelibrary.wiley.com/terms-and-conditions) on Wiley Online Library for rules of use; OA articles are governed by the applicable Creative Commons License